Article

Urban Resilience of Important Node Cities in Population Migration under the Influence of COVID-19 Based on Mamdani Fuzzy Inference System

Huilong Wang [1], Meimei Wang [2], Rong Yang [1,*] and Huijuan Yang [1]

[1] School of Geography and Planning, Ningxia University, Yinchuan 750021, China; wanghl036@163.com (H.W.); yanghj0507@163.com (H.Y.)
[2] College of Earth and Environmental Sciences, Lanzhou University, Lanzhou 730000, China; wangmm@lzu.edu.cn
[*] Correspondence: yangr821@163.com

Abstract: COVID-19 has resulted in a great inconvenience and has had a severe impact on the economy and residents' daily life in China and even the world. Urban resilience, as the key representation of social and economic stability, can directly reflect the development and stability of cities. In addition, the Mamdani fuzzy inference system (MFIS), as one of the commonly used fuzzy inference systems, has been successfully applied in various application problems involving imprecise or vague information since it was proposed. In this paper, we mainly consider the urban resilience of 50 important node cities for population migration (50INCPM) in China in 2020 under the influence of COVID-19. We apply MFIS for approximating the urban resilience index (URI) based on multiple inputs, which includes the population density resilience index (PRI), gross domestic product per capita resilience index (GRI), in-degree centrality resilience index (IRI), out-degree centrality resilience index (ORI), confirmed cases number (CCN), recovery rate (RR) and mortality rate (MR). Meanwhile, based on the big data of population migration and COVID-19 data in China from 15 January to 15 March in 2020, we calculate the URI of 50INCPM in China in 2020 under the influence of COVID-19. Moreover, we show the spatial difference of URI and its changes in different stages. The results show that (1) the URI of 50INCPM decreases from the eastern coastal area to the western inland, and the cities with URI more than 0.5 are gathered in the eastern coastal area of China. As COVID-19 is controlled, the URI is gradually rising, and the growth rate of URI in southeast coastal cities exceeds that of inland cities. (2) The second-tier and third-tier cities have stronger resilience in the case of large-scale emergencies. (3) There exists a positive correlation in URI and RR. The expectation of the research finding gives a basis for judging the economic and social situation under the impact of COVID-19, which can help local governments accurately judge city resilience, and provide a reference for the decision on resuming production and work, so it is of positive significance for national economic resilience and social stability. Finally, on the basis of universal vaccine coverage, we hold that the GOC should promote the cities' resilience in China, especially in the first-tier city in inland China (Beijing, Shanghai, Guangzhou and Shenzhen). On the other hand, on the premise of implementing epidemic prevention and control measures, local governments should stimulate the resilience of each city in terms of population and economy.

Keywords: urban resilience; node cities; population migration; COVID-19; mamdani fuzzy inference system

1. Introduction

Since December of 2019, many hospitals in Wuhan in Hubei Province of China have found many cases with unknown pneumonia, which have manifested as fever, dry cough and fatigue [1]. Meanwhile, middle-aged and elderly people are more likely to become

infected and develop severe symptoms [2], due to damage to the lungs, liver and blood-clotting system [3]. This incident immediately attracted the world's attention, and subsequently, the World Health Organization (WHO) announced this unknown pneumonia as Corona Virus Disease 2019 (COVID-19) on 11 February 2020. On 11 March 2020, the WHO decided that the COVID-19 outbreak could be deemed a global pandemic [4]. Different from some governments in other countries framing COVID-19 as affecting only certain sub-groups severely in government narratives [5], the government of China (GOC) adopted the strictest intercity travel restrictions to prevent further seeding of the virus in China [6]. Since mid-March of 2020, the outbreak of COVID-19 in China appeared to be contained [7]. But the diffusion of COVID-19 in Europe and United States has begun to get worse since April of 2020 [8].

On 15 January 2020, the National Health Commission of China (http://www.nhc.gov.cn (accessed on 9 August 2023)) began to publish the pandemic data in each city of China, which included the confirmed cases number (CCN), recovery number, and mortality number every day in each city of China. Until 1 November 2021, the cumulative number of CCN was 97,314, the cumulative recovery number was 91,766, and the cumulative mortality number was 4636; see Figure 1.
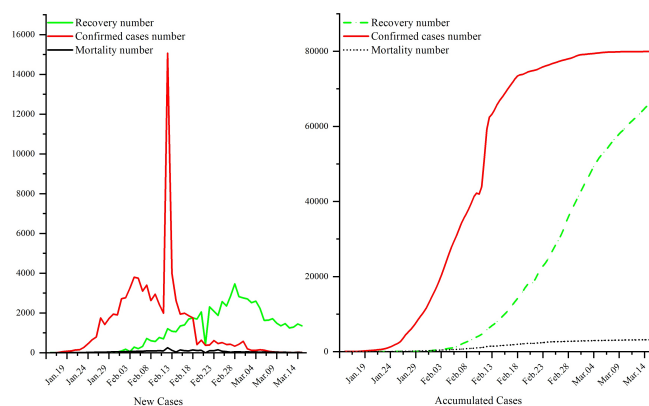
Figure 1. The situation of COVID-19 in China.

COVID-19 has had a huge impact on the economic activities [9], production and peoples' daily lives [10] around the world. From the perspective of external international influence, the impact of COVID-19 on China's economy has shown a glide in international trade, cross-border tourism and other industries in the short term [11], and it has strengthened risk aversion in the short-term market as well [8]. Overall, the impact of COVID-19 on China's capital market is more profound than that of SARS (severe acute respiratory syndrome in 2003), which has exacerbated short-term fluctuations in the capital market [12]. Similarly, the COVID-19 pandemic has had a negative impact on markets and society, in particular, within the stock market of the United States [13]. Domestically, COVID-19 causes a short-term external impact for the domestic macro economy. What is more serious is that COVID-19 has caused a huge impact on the individual work, communication, daily life and mental condition [14]. Moreover, COVID-19 is a highly complex multi-issue crisis [15]. This external impact has inevitably interfered with China's economic growth, led to social and public health crises and then resulted in social crisis and psychological crisis. As far as residents are concerned, markets and supply chains have been disrupted, and millions of people have lost their jobs and livelihoods [16]. COVID-19 has changed people's daily activities and challenged people to adjust their life styles to accommodate the need for social distance [17]. On the whole, COVID-19 has disrupted developing countries' economy in particular [16]. Meanwhile, there is a certain degree of uncertainty in prevention, which has increased the difficulty in prevention.

It is indisputable that COVID-19 has brought a huge impact on the world economy and social stability [18]. This impact directly has a negative impact on the normal operation

and healthy development of a city. Over the past few years, there has been a proliferation of studies that focus on enhancing urban resilience against a multitude of man-made and natural disasters [19]. Based on the improved gravity algorithm, the influence of the logistics spatial connection between node cities is analyzed. The decrease in logistics level and confirmed cases showed the same spatial variation law. Wuhan city experienced the most severe decline in logistics levels and spatial connectivity [20]. The logistics level and spatial connection of Wuhan are the most seriously declined. The decline in logistics level has the same spatial variation law as the confirmed cases. There has also been an increase in the number of frameworks and tools developed for assessing urban resilience. The present study has not obtained a consensus conclusion on the impact of city size on COVID-19. Those who favor megacities consider that urban governance capacity is an important factor affecting the prevention and control of the COVID-19 pandemic, and urban governance capacity was particularly significant in the late control of the COVID-19 outbreak [21], so Chinese cities need to continue to scale up and take advantage of large-city governance [22]. Small- and medium-sized city advocates believe that the COVID-19 pandemic hit hard mostly in large- and medium-sized cities, and larger metropolitan areas have had higher infection and higher mortality rates [23]. GIS methods have been used in order to estimate and visualize the ongoing COVID-19 pandemic situation, and the trajectory of the virus paths was estimated. Sparsely populated areas with poorly developed and small traffic networks tend to be less or not affected [24].

On the other hand, fuzzy logic is much closer in spirit to human thinking and natural language than the classical logical systems. Basically, it provides an effective means of capturing the approximate, inexact nature of the real world. In particular, the fuzzy logic is useful in the case that the available sources of information are interpreted qualitatively, inexactly, or uncertainly. In addition, the fuzzy inference system (FIS), developed based on fuzzy logic as a powerful tool and model to help decision makers deal with practical application problems through approximate reasoning and linguistic terminology, uses fuzzy "if–then" rules to model the qualitative aspects of human knowledge without using any precise quantitative analysis. And thus, when using FIS to deal with practical application problems involving inaccuracies in the collected data, it is often much better than using other models.

In the context of the epidemic, as urban resilience research is becoming a major scientific issue affecting and restricting the sustainable development of modern cities, a scientific theoretical system is urgently needed to analyze the urban resilience characteristics and construction issues at different spatial scales and regions [25]. Meanwhile, building an urban resilience assessment framework comprehensive assessment of the urban resilience building status and development can promote healthy and stable urban development [26]. Thus, the exploration of urban resilience in different cities under the impact of the COVID-19 pandemic is necessary. Concurrently, indexes of urban resilience can be divided into society and well-being, built environment and infrastructure, environmental resources and economy, etc. At present, the measurement and evaluation methods of urban resilience are discussed. Most of them adopt qualitative methods; mainly on the basis of screening key indicators, the function model method of analyzing the coping ability, the comprehensive index method based on the factor weight calculation, the principal component analysis method and the graph overlay method combined with GIS were used for comprehensive evaluation. The extent to which a city responds to external threats cannot be clearly calculated [27]. Intuitively, the impact of COVID-19 on the built environment and environmental resources is not obvious. As population movement restrictions are considered to be one of the main policies to curb the spread of COVID-19 [28], the impact of COVID-19 on population mobility is self-evident. Therefore, in order to calculate the URI of cities, we use the PRI and GRI to reflect the impact of COVID-19 on society and economy, IRI and ORI to characterize the changes in population mobility under COVID-19, and CCN, RR, and MR of COVID-19 to show the situation of COVID-19 in this paper. And we propose a method on the basis of MFIS, which is one of the most commonly used FIS. Beyond those,

the evaluation of urban resilience of important node cities for population migration can judge the economic and social situation under the impact of COVID-19. It can help local governments accurately judge the resilience in a city, and provide reference for GOC to make relevant plans to resume production and work, so it is of positive significance for national economic resilience and social stability [29,30].

Therefore, in this paper, we focus on the evaluation of urban resilience of 50INCPM in China in 2020 under the influence of COVID-19. Specifically, we focus on solving the following problems.

(i) **How is the resilience of 50INCPM in China in 2020 under the influence of COVID-19?**
(ii) **In the case of large-scale emergencies, which has stronger resilience, metropolises or small cities?**

2. Data Sources and Study Area

2.1. Data Sources

Data in this paper were obtained from big data of migration of Baidu http://qianxi.baidu.com (accessed on 9 August 2023) from 15 January 2020 to 15 March 2020, and the National Health Commission of China (http://www.nhc.gov.cn (accessed on 9 August 2023) in 2020. Because population migration can reflect the economic and social development of a city, we select population inflow and outflow data to reflect the population migration in important node cities in population migration. Furthermore, the flow of population in different periods can reflect the economic and social conditions at different times. As for COVID-19 data, CCN, RR and MR of COVID-19 are selected to reflect the situation.

2.2. Study Period Selection

We selected 15 January 2020 (the first day that the National Health Commission announced the number of COVID-19 cases) to 15 March 2020 (COVID-19 in China appears to be contained) as the research period, a total of 60 days. The period includes 24–31 January 2020 (traditional China's New Year's Eve and Spring Festival holidays), 3 February (the first working day of the New Year), 52 February (first peak number of CCN of COVID-19, 3694 in a day), and 12 February (highest peak of CCN of COVID-19, 15,152 in a day). This study period can be divided into three stages.

(1) The incubative period: This period is from 15 January to 31 January 2020.
(2) The pandemic period: This period is from 1 February 2020 to 20 February 2020.
(3) The controlled period: This period is from 21 February 2020 to 15 March 2020.

2.3. The Study Area Selection

By calculating the total migration degree and migration intensity of population flow in municipal cities in China in the study period, we select 50INCPM in 2020 as the study areas. These 50 cities are ranked based on the total migration degree and migration intensity of population flow. To a large extent, they can represent the direction and pattern of urban population flow in mainland China under the influence of COVID-19. The distribution of important node cities for population migration is decreasing from the eastern coast to the western inland, mainly concentrated in Guangdong, Zhejiang, Jiangsu and Shandong provinces. These cities have obvious agglomeration and radiation. They have a relatively concentrated population in a larger region, a relatively strong comprehensive strength, and a strong ability to attract, radiate and provide comprehensive services in politics, economy, culture and other aspects. They are economically developed and can drive and organize the economic development of the surrounding region, which is of great attraction to other cities in the region.

The total migration degree and migration intensity of population flow from 15 January 2020 to 15 March 2020 is obtained through complex network methods, and the total migration degree and migration intensity of the population flow in municipal cities are shown in Figure 2 (the map approval number is GS(2019)1822). From Figure 2, 50INCPM in 2020 are Chengdu, Beijing, Guangzhou, Shenzhen, Shanghai, Dongguan, Xian, Chongqing, Suzhou,

Xiangxi, Qingyuan, Hangzhou, Foshan, Shaoguan, Zhengzhou, Changsha, Kunming, Nanjing, Shantou, Heze, Tianjin, Suqian, Wuxi, Hefei, Guiyang, Suihua, Jinan, Enshi, Xianyang, Langfang, Zhaoqing, Shangrao, Huizhou, Ningbo, Xuzhou, Wenzhou, Haerbin, Zhoukou, Zhongshan, Qingdao, Fuzhou, Changzhou, Shaoxing, Wuhan, Nanning, Jiaxing, Handan, Lishui, Linyi, and Weifang.
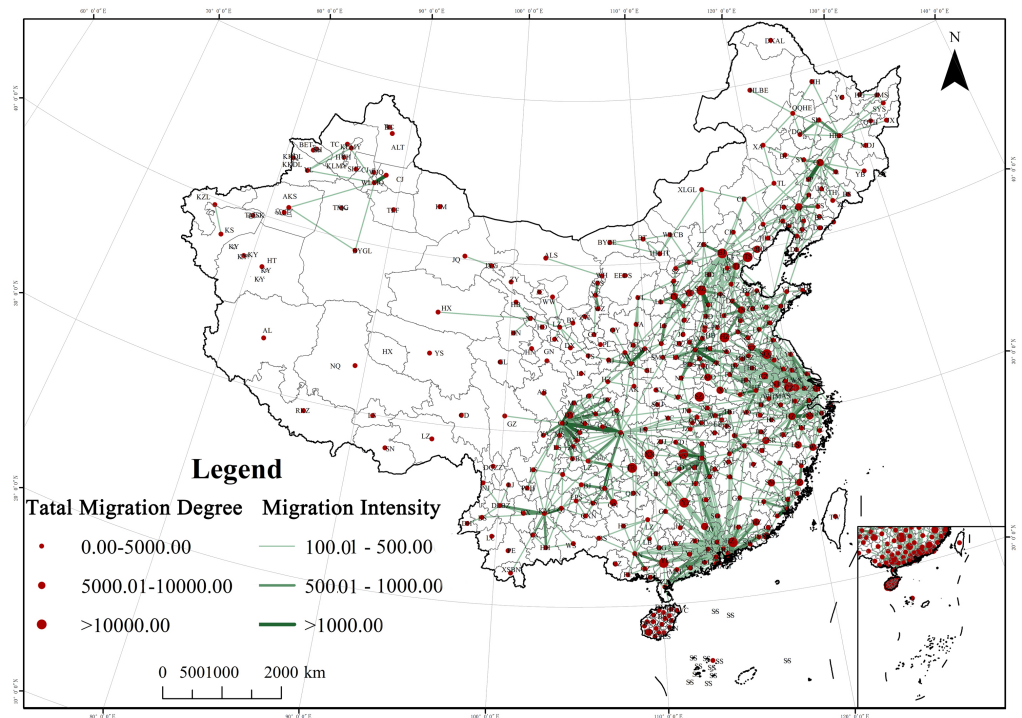
Figure 2. The total migration degree and migration intensity of population flow in municipal cities of China.

3. Proposed Method

MFIS, as a systematic formulation of pre-defined "if–then" rules, was introduced by Mamdani and Assilian in [31] to interpret human perceptions and has been successfully applied in various application problems. In particular, recently, Ghosh and Biswas [32] used a generated MFIS to successfully quantify all Indian states and autonomous regions in preventing the COVID-19 pandemic situation. Inspired by these, in this section, we show a method on the basis of MFIS to calculate the URI of the top 50 important node cities for population migration in China during 2020 under the influence of COVID-19. Meanwhile, in order to illustrate the proposed method, we show a flowchart in Figure 3.

In addition, it should be pointed out that all the crisp inputs for the proposed method are fuzzified into triangular fuzzy numbers (TFNs). Properly speaking, for a crisp input α of the proposed method, it is fuzzified into the TFN shown as follows:

$$A_\alpha = \langle (1-\delta)\alpha, \alpha, (1+\delta)\alpha \rangle \tag{1}$$

with the membership function as

$$\mu_{A_\alpha}(x) = \begin{cases} \frac{x-(1-\delta)\alpha}{\alpha\delta} & \text{if } (1-\delta)\alpha \leq x \leq \alpha, \\ \frac{(1+\delta)\alpha-x}{\alpha\delta} & \text{if } \alpha \leq x \leq \alpha(1+\delta), \\ 0 & \text{otherwise} \end{cases} \tag{2}$$

where $\delta > 0$. And, the reasons for this are stated below.

- The data are collected from big data of the migration of Baidu (http://qianxi.baidu.com (accessed on 9 August 2023) and the National Health Commission of China (http://www.nhc.gov.cn (accessed on 9 August 2023). So, the input parameters PRI, IRI, ORI, GRI, RR, CCN and MR are inevitably inaccurate in the data statistics process, that is, the obtained data have a certain degree of uncertainty. Therefore, it is particularly important and necessary to fuzzify the data. At the same time, it must be mentioned that this fuzzification method was successfully applied in solving problems related to COVID-19, see, for example, the recent works [33–47].
- Due to the vast territory of China, there may be some omissions and inconsistent measurement rules when reporting data from different cities. Therefore, the input data we collected may have some slight omissions and inconsistencies. These omissions and inconsistencies generally do not affect the overall description, and can reflect the relevant situation of the economic and social indicators of the corresponding city under the influence of COVID-19. However, in order to balance these slight omissions and inconsistencies, all the crisp inputs are fuzzified into TFNs in our methodology.
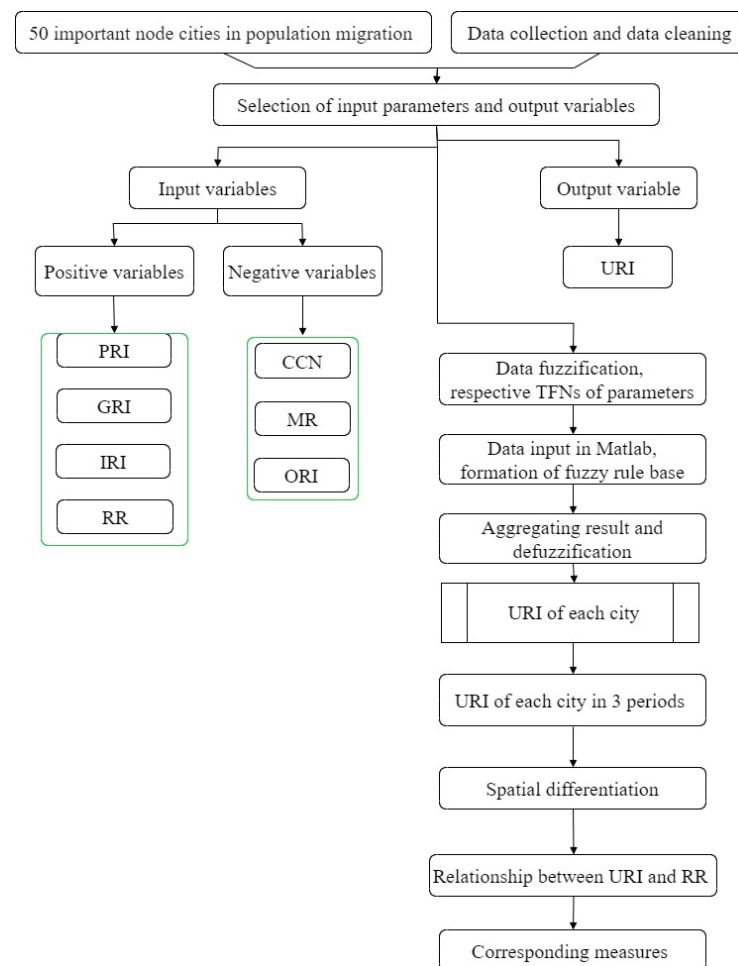
Figure 3. The proposed method workflow.

The proposed method is described as follows:

- **Step 1: Variables selection**
  The used MFIS consists of seven input variables and one output variable. Specifically, the seven input variables are PRI, IRI, ORI, GRI, RR, CCN, and MR in the universe of discourses X_1, X_2, X_3, X_4, X_5, X_6, and X_7, respectively, and one output variable is URI in the universe of discourse Y. In order to capture the uncertainty associated with the

collected data, the membership functions (MFs) of the input and output variables are both represented by TFNs.

- **Step 2: Rule base**

  The rule base of MFIS depicts the relationship between input and output variables. The ith $(i = 1, 2, \cdots, n)$ "if–then" rule of a MFIS is taken through the following format:

  $$R_i : \text{ If } x_1 \text{ is } F^i_{PRI} \text{ and } x_2 \text{ is } F^i_{IRI} \text{ and } x_3 \text{ is } F^i_{ORI}$$

  $$\text{and } x_4 \text{ is } F^i_{GRI} \text{ and } x_5 \text{ is } F^i_{RR} \text{ and } x_6 \text{ is } F^i_{CCN}$$

  $$\text{and } x_7 \text{ is } F^i_{MR}, \text{ then } y \text{ is } F^i_{URI},$$

  where $x_1, x_2, x_3, x_4, x_5, x_6, x_7$ and y belong to $X_1, X_2, X_3, X_4, X_5, X_6, X_7$ and Y, respectively, and $F^i_{PRI}, F^i_{IRI}, F^i_{ORI}, F^i_{GRI}, F^i_{RR}, F^i_{CCN}, F^i_{MR}$ and F^i_{URI} are TFNs used to represent the qualitative description of PRI, IRI, ORI, GRI, RR, CCN, MR and URI, respectively.

- **Step 3: Calculate the fire strength of apiece rule**

  In the large amount of existing work (see, for example, [32,48]), the fuzzy intersection operation, as the most commonly used logical connective in fuzzy logic, is widely used to evaluate the fire strength of each rule. So, here, we also use the fuzzy intersection operation to evaluate the fire strength of ith $(i = 1, 2, \cdots, n)$ rule β_i, and the details are listed as follows:

  $$\begin{aligned}
  \beta_i = \max & \left\{ \min \left\{ \mu_{F^i_{PRI}}(x), \mu_{G_{PRI}}(x) \right\} : x \in X_1 \right\} \\
  & \wedge \max \left\{ \min \left\{ \mu_{F^i_{IRI}}(x), \mu_{G_{IRI}}(x) \right\} : x \in X_2 \right\} \\
  & \wedge \max \left\{ \min \left\{ \mu_{F^i_{ORI}}(x), \mu_{G_{ORI}}(x) \right\} : x \in X_3 \right\} \\
  & \wedge \max \left\{ \min \left\{ \mu_{F^i_{GRI}}(x), \mu_{G_{GRI}}(x) \right\} : x \in X_4 \right\} \\
  & \wedge \max \left\{ \min \left\{ \mu_{F^i_{RR}}(x), \mu_{G_{RR}}(x) \right\} : x \in X_5 \right\} \\
  & \wedge \max \left\{ \min \left\{ \mu_{F^i_{CCN}}(x), \mu_{G_{CCN}}(x) \right\} : x \in X_6 \right\} \\
  & \wedge \max \left\{ \min \left\{ \mu_{F^i_{MR}}(x), \mu_{G_{MR}}(x) \right\} : x \in X_7 \right\},
  \end{aligned} \tag{3}$$

  where $\mu_{F^i_{PRI}}, \mu_{F^i_{IRI}}, \mu_{F^i_{ORI}}, \mu_{F^i_{GRI}}, \mu_{F^i_{RR}}, \mu_{F^i_{CCN}}$ and $\mu_{F^i_{MR}}$ are the MFs of fuzzy sets $F^i_{PRI}, F^i_{IRI}, F^i_{ORI}, F^i_{GRI}, F^i_{RR}, F^i_{CCN}$ and F^i_{MR} of qualitative descriptors in rule R_i, respectively, and $\mu_{G_{PRI}}, \mu_{G_{IRI}}, \mu_{G_{ORI}}, \mu_{G_{GRI}}, \mu_{G_{RR}}, \mu_{G_{CCN}}$ and $\mu_{G_{MR}}$ are the MFs of fuzzy inputs $G_{PRI}, G_{IRI}, G_{ORI}, G_{GRI}, G_{RR}, G_{CCN}$ and G_{MR} in the form of TFNs, respectively.

- **Step 4: Derivation of fuzzy output of each rule**

  In the abundant existing work (see, for example, [32,48,49]), the output of apiece i^{th} $(i = 1, 2, \cdots, n)$ rule R_i is taken as the intersection of the fire strength of rule R_i and the MF of the qualitative descriptor for the corresponding output. Therefore, here, we also use the intersection operation to derive the fuzzy output of the ith $(i = 1, 2, \cdots, n)$ rule as follows:

  $$v_{F^i_{URI}}(y) = \min \left\{ \beta_i, \mu_{F^i_{URI}}(y) \right\} \tag{4}$$

  where β_i is the fire strength of rule R_i, $\mu_{F^i_{URI}}$ is the MF of F^i_{URI} (the qualitative descriptor of the output URI), and $y \in Y$.

- **Step 5: Aggregation of fuzzy outputs**

  Just like the method used in various existing works in the literature (see, for example, [32,48,49]), we adopt the fuzzy union operation to aggregate the output of the ith $(i = 1, 2, \cdots, n)$ rule R_i as follows:

  $$v_{F_{URI}}(y) = \max \left\{ v_{F^1_{URI}}(y), v_{F^2_{URI}}(y), \cdots, v_{F^n_{URI}}(y) \right\} \tag{5}$$

where $v_{F_{URI}^i}$ is the MF of the derived fuzzy output of the ith $(i = 1, 2, \cdots, n)$ rule, n is the sum total of rules in the rule base, and $y \in Y$.

- **Step 6: Defuzzification of the aggregated output**
  As is well known, the centroid-of-area method, as a way to determine the center of gravity of an aggregated fuzzy set, has been successfully applied in various works (see, for example, [32,50]) to defuzzify the aggregated output. And, here, we also use the centroid-of-area method to defuzzify the aggregated output and obtain the final output URI as follows:

$$
URI = \frac{\sum_{j=1}^{k} y_j \cdot v_{F_{URI}}(y_j)}{\sum_{j=1}^{k} v_{F_{URI}}(y_j)}, \tag{6}
$$

where $y_j \in Y$ are k quantization of Y.

4. URI of Important Node Cities for Population Migration under the Influence of COVID-19

The PRI, GRI, IRI, ORI, CCN, RR and MR are set as input variables, and URI is set as the output variable in calculation. In this section, we describe these variables and give their respective TFNs to represent the linguistic hedges according to low, medium and high. First, we perform fuzzification on the overall values of all input parameters, and the results are shown in Table 1.

4.1. Membership Functions for Input and Output Parameters

PRI: the average population density resilience index. According to the China urban statistical yearbook in 2019 and 2020, the average population density resilience index (PRI) of 50INCPM in 2020 was 1.2610. Foshan's PRI is the largest; it is 2.5609. Xiangxi's PRI is the smallest; it is 0.1016. Thus, we use the TFNs $\langle 0, 0, 1.2610 \rangle$, $\langle 0.522, 1.2610, 2 \rangle$ and $\langle 1.2610, 3, 3 \rangle$ to express the language fuzzy constraints for low, medium and high PRI, respectively; see Figure 4.

GRI: the average gross domestic product per capita resilience index. The gross domestic product per capita in 50INCPM in 2019 was CNY 15.7446 thousand and CNY 16.6553 thousand in 2020.Thus, the average gross domestic product per capita resilience index (GRI) in 2020 of 50INCPM is 1.0667. Xiangxi's GRI is the largest; it is 1.6670. Langfang's GRI is the smallest; it is 0.7149. Thus, we use the TFNs $\langle 0, 0, 1.0667 \rangle$, $\langle 0.8334, 1.0667, 1.300 \rangle$ and $\langle 1.0667, 1.75, 1.75 \rangle$ to express the language fuzzy constraints for low, medium and high GRI, respectively; see Figure 5.

IRI: the average in-degree centrality resilience index. According to big data of the migration of Baidu, the average in-degree centrality resilience index (IRI) of 50INCPM was 3.2023 in 2019 and it was 1.7499 in 2020. So the IRI of 50INCPM is 0.5759. Among them, Jinan's IRI is the largest; it is 0.7363. Wuhan's IRI is the smallest; it is 0.1643. Thus, we use the TFNs $\langle 0, 0, 0.5759 \rangle$, $\langle 0.4500, 0.5759, 0.75 \rangle$ and $\langle 0.5759, 1.300, 1.300 \rangle$ to express the language fuzzy constraints for low, medium and high of IRI, respectively; see Figure 6.

ORI: the out-degree centrality resilience index. According to the big data of migration of Baidu, the out-degree centrality resilience index (ORI) of 50INCPM was 3.0724 in 2019 and 1.8338 in 2020, that is, the average ORI of 50INCPM is 0.5874. Changzhou's ORI is the largest; it is 0.7266. Wuan's ORI is the smallest; it is 0.3448. Thus, we use the TFNs $\langle 0, 0, 0.5874 \rangle$, $\langle 0.474, 0.5874, 0.70 \rangle$ and $\langle 0.5874, 1.300, 1.300 \rangle$ to express language fuzzy constraints for low, medium and high ORI, respectively; see Figure 7.

Table 1. The fuzzified input values of the selected top 50 important node cities.

City	PRI	GRI	ORI	IRI	CCN	MR	RR
Chengdu	⟨1.2258, 1.2508, 1.2758⟩	⟨1.0588, 1.0804, 1.1020⟩	⟨0.5980, 0.6102, 0.6225⟩	⟨0.5109, 0.5214, 0.5318⟩	⟨2.3134, 2.3607, 2.4079⟩	⟨0.0204, 0.0208, 0.0213⟩	⟨0.8303, 0.8472, 0.8642⟩
Beijing	⟨1.0236, 1.0445, 1.0654⟩	⟨1.1478, 1.1712, 1.1947⟩	⟨0.5579, 0.5693, 0.5807⟩	⟨0.4514, 0.4606, 0.4698⟩	⟨7.1010, 7.2459, 7.3908⟩	⟨0.0177, 0.0181, 0.0185⟩	⟨0.7827, 0.7986, 0.8146⟩
Guangzhou	⟨1.1728, 1.1967, 1.2206⟩	⟨0.9859, 1.0060, 1.0261⟩	⟨0.5400, 0.5511, 0.5621⟩	⟨0.4680, 0.4776, 0.4871⟩	⟨5.5908, 5.7049, 5.8190⟩	⟨0.0028, 0.0029, 0.0029⟩	⟨0.9293, 0.9483, 0.9672⟩
Shenzhen	⟨0.7940, 0.8103, 0.8265⟩	⟨1.0520, 1.0734, 1.0949⟩	⟨0.6248, 0.6375, 0.6503⟩	⟨0.6477, 0.6609, 0.6742⟩	⟨6.7797, 6.9180, 7.0564⟩	⟨0.0070, 0.0071, 0.0073⟩	⟨0.9266, 0.9455, 0.9644⟩
Shanghai	⟨0.6679, 0.6815, 0.6952⟩	⟨1.1419, 1.1652, 1.1885⟩	⟨0.6133, 0.6258, 0.6383⟩	⟨0.5318, 0.5427, 0.5535⟩	⟨5.7033, 5.8197, 5.9361⟩	⟨0.0083, 0.0085, 0.0086⟩	⟨0.8944, 0.9127, 0.9309⟩
Dongguan	⟨0.8564, 0.8739, 0.8914⟩	⟨1.1144, 1.1371, 1.1599⟩	⟨0.6345, 0.6475, 0.6604⟩	⟨0.5943, 0.6064, 0.6186⟩	⟨1.6066, 1.6393, 1.6721⟩	⟨0.0098, 0.0100, 0.0102⟩	⟨0.9506, 0.9700, 0.9894⟩
Xian	⟨1.2119, 1.2366, 1.2614⟩	⟨0.9415, 0.9607, 0.9799⟩	⟨0.4925, 0.5025, 0.5126⟩	⟨0.4827, 0.4926, 0.5024⟩	⟨1.9279, 1.9672, 2.0066⟩	⟨0.0163, 0.0167, 0.0170⟩	⟨0.8983, 0.9167, 0.9350⟩
Chongqing	⟨1.0950, 1.1173, 1.1397⟩	⟨1.1207, 1.1435, 1.1664⟩	⟨0.6609, 0.6744, 0.6878⟩	⟨0.6809, 0.6948, 0.7087⟩	⟨9.2538, 9.4426, 9.6315⟩	⟨0.0102, 0.0104, 0.0106⟩	⟨0.9698, 0.9896, 1.0094⟩
Suzhou	⟨1.2726, 1.2986, 1.3245⟩	⟨1.0060, 1.0265, 1.0470⟩	⟨0.5505, 0.5618, 0.5730⟩	⟨0.6661, 0.6797, 0.6933⟩	⟨1.3977, 1.4262, 1.4548⟩	⟨0.0000, 0.0000, 0.0000⟩	⟨0.9800, 1.0000, 1.0200⟩
Xiangxi	⟨0.0996, 0.1016, 0.1037⟩	⟨1.6345, 1.6679, 1.7012⟩	⟨0.6093, 0.6217, 0.6341⟩	⟨0.5245, 0.5352, 0.5459⟩	⟨0.1285, 0.1311, 0.1338⟩	⟨0.0000, 0.0000, 0.0000⟩	⟨0.9800, 1.0000, 1.0200⟩
Qingyuan	⟨1.3609, 1.3887, 1.4165⟩	⟨1.0556, 1.0771, 1.0987⟩	⟨0.6986, 0.7129, 0.7272⟩	⟨0.6203, 0.6330, 0.6456⟩	⟨0.1928, 0.1967, 0.2007⟩	⟨0.0000, 0.0000, 0.0000⟩	⟨0.9800, 1.0000, 1.0200⟩
Hangzhou	⟨1.6932, 1.7278, 1.7623⟩	⟨1.0686, 1.0904, 1.1122⟩	⟨0.4684, 0.4780, 0.4876⟩	⟨0.5558, 0.56710.5785⟩	⟨2.9239, 2.9836, 3.0433⟩	⟨0.0000, 0.0000, 0.0000⟩	⟨0.9638, 0.9835, 1.0032⟩
Foshan	⟨2.5097, 2.5609, 2.6121⟩	⟨1.0273, 1.0482, 1.0692⟩	⟨0.5582, 0.5695, 0.5809⟩	⟨0.5288, 0.5396, 0.5504⟩	⟨1.3656, 1.3934, 1.4213⟩	⟨0.0000, 0.0000, 0.0000⟩	⟨0.9339, 0.952, 0.9720⟩
Shaoguan	⟨1.2510, 1.2765, 1.3021⟩	⟨0.9367, 0.9558, 0.9749⟩	⟨0.6126, 0.6251, 0.6376⟩	⟨0.5830, 0.5949, 0.6068⟩	⟨0.1607, 0.1639, 0.1672⟩	⟨0.0980, 0.1000, 0.1020⟩	⟨0.8820, 0.9000, 0.9180⟩
Zhengzhou	⟨0.9753, 0.9952, 1.0151⟩	⟨1.2612, 1.2870, 1.3127⟩	⟨0.5645, 0.5761, 0.5876⟩	⟨0.5904, 0.6024, 0.6145⟩	⟨2.5223, 2.5738, 2.6252⟩	⟨0.0312, 0.0318, 0.0325⟩	⟨0.9488, 0.9682, 0.9875⟩
Changsha	⟨0.8841, 0.9021, 0.9202⟩	⟨0.9889, 1.0091, 1.0292⟩	⟨0.5983, 0.6105, 0.6227⟩	⟨0.5225, 0.5332, 0.5439⟩	⟨3.8879, 3.9672, 4.0466⟩	⟨0.0081, 0.0083, 0.0084⟩	⟨0.9719, 0.9917, 1.0116⟩
Kunming	⟨0.7663, 0.7820, 0.7976⟩	⟨1.1892, 1.2135, 1.2377⟩	⟨0.3536, 0.3609, 0.3681⟩	⟨0.5641, 0.5757, 0.5872⟩	⟨0.8515, 0.8689, 0.8862⟩	⟨0.0000, 0.0000, 0.0000⟩	⟨0.9800, 1.0000, 1.0200⟩
Nanjing	⟨1.1136, 1.1363, 1.1590⟩	⟨1.0620, 1.0837, 1.1054⟩	⟨0.6232, 0.6359, 0.6486⟩	⟨0.6714, 0.6851, 0.6988⟩	⟨1.4941, 1.5246, 1.5551⟩	⟨0.0000, 0.0000, 0.0000⟩	⟨0.9800, 1.0000, 1.0200⟩
Shantou	⟨1.6738, 1.7080, 1.7421⟩	⟨1.0446, 1.0659, 1.0872⟩	⟨0.6046, 0.6170, 0.6293⟩	⟨0.6713, 0.6850, 0.6987⟩	⟨0.4016, 0.4098, 0.4180⟩	⟨0.0000, 0.0000, 0.0000⟩	⟨0.9408, 0.9600, 0.9792⟩
Heze	⟨2.3023, 2.3493, 2.3963⟩	⟨1.1955, 1.2199, 1.2443⟩	⟨0.5068, 0.5172, 0.5275⟩	⟨0.5941, 0.6062, 0.6183⟩	⟨0.2892, 0.2951, 0.3010⟩	⟨0.0000, 0.0000, 0.0000⟩	⟨0.9800, 1.0000, 1.0200⟩
Tianjin	⟨0.9423, 0.9615, 0.9808⟩	⟨0.7337, 0.7487, 0.7636⟩	⟨0.5859, 0.5978, 0.6098⟩	⟨0.5252, 0.5359, 0.5466⟩	⟨2.1849, 2.2295, 2.2741⟩	⟨0.0216, 0.0221, 0.0225⟩	⟨0.9584, 0.9779, 0.9975⟩
Suqian	⟨1.0434, 1.0647, 1.0860⟩	⟨1.0692, 1.0910, 1.1129⟩	⟨0.6134, 0.6259, 0.6385⟩	⟨0.6485, 0.6618, 0.6750⟩	⟨0.2089, 0.2131, 0.2174⟩	⟨0.0000, 0.0000, 0.0000⟩	⟨0.9800, 1.0000, 1.0200⟩
Wuxi	⟨1.3062, 1.3328, 1.3595⟩	⟨1.0022, 1.0227, 1.0431⟩	⟨0.6121, 0.6246, 0.6371⟩	⟨0.5070, 0.5173, 0.5277⟩	⟨0.8836, 0.9016, 0.9197⟩	⟨0.0000, 0.0000, 0.0000⟩	⟨0.9800, 1.0000, 1.0200⟩
Hefei	⟨1.1722, 1.1961, 1.2200⟩	⟨1.1716, 1.1955, 1.2194⟩	⟨0.5147, 0.5252, 0.5357⟩	⟨0.4610, 0.4704, 0.4798⟩	⟨2.7954, 2.8525, 2.9095⟩	⟨0.0056, 0.0057, 0.0059⟩	⟨0.9744, 0.9943, 1.0141⟩
Guiyang	⟨1.2720, 1.2980, 1.3239⟩	⟨1.0837, 1.1058, 1.1280⟩	⟨0.5022, 0.5124, 0.5226⟩	⟨0.5718, 0.5834, 0.5951⟩	⟨0.5784, 0.5902, 0.6020⟩	⟨0.0272, 0.0278, 0.0283⟩	⟨0.9256, 0.9444, 0.9633⟩
Suihua	⟨1.0193, 1.0401, 1.0609⟩	⟨1.0685, 1.0903, 1.1121⟩	⟨0.6259, 0.6387, 0.6515⟩	⟨0.6905, 0.7046, 0.7187⟩	⟨0.7551, 0.7705, 0.7859⟩	⟨0.0834, 0.0851, 0.0868⟩	⟨0.8549, 0.8723, 0.8898⟩
Jinan	⟨1.5744, 1.6065, 1.6387⟩	⟨0.9358, 0.9549, 0.9740⟩	⟨0.5864, 0.5984, 0.6104⟩	⟨0.7215, 0.7363, 0.7510⟩	⟨0.7551, 0.7705, 0.7859⟩	⟨0.0000, 0.0000, 0.0000⟩	⟨0.9591, 0.9787, 0.9983⟩
Enshi	⟨1.3434, 1.3709, 1.3983⟩	⟨1.1301, 1.1532, 1.1762⟩	⟨0.5467, 0.5578, 0.5690⟩	⟨0.7059, 0.7203, 0.7347⟩	⟨4.0485, 4.1311, 4.2138⟩	⟨0.0272, 0.0278, 0.0283⟩	⟨0.9372, 0.9563, 0.9755⟩
Xianyang	⟨1.1001, 1.1225, 1.1450⟩	⟨0.9211, 0.9399, 0.9587⟩	⟨0.5964, 0.6086, 0.6208⟩	⟨0.6260, 0.6387, 0.6515⟩	⟨0.2731, 0.2787, 0.2843⟩	⟨0.0000, 0.0000, 0.0000⟩	⟨0.9224, 0.9412, 0.9600⟩
Langfang	⟨0.9482, 0.9676, 0.9869⟩	⟨0.7006, 0.7149, 0.7292⟩	⟨0.5424, 0.5535, 0.5646⟩	⟨0.5339, 0.5448, 0.5557⟩	⟨0.4820, 0.4918, 0.5016⟩	⟨0.0000, 0.0000, 0.0000⟩	⟨0.9800, 1.0000, 1.0200⟩
Zhaoqing	⟨1.3656, 1.3935, 1.4213⟩	⟨0.9835, 1.0035, 1.0236⟩	⟨0.4998, 0.5100, 0.5202⟩	⟨0.5248, 0.5355, 0.5462⟩	⟨0.3052, 0.3115, 0.3177⟩	⟨0.0516, 0.0526, 0.0537⟩	⟨0.9284, 0.9474, 0.9663⟩
Shangrao	⟨0.8318, 0.8487, 0.8657⟩	⟨0.9431, 0.9623, 0.9816⟩	⟨0.5799, 0.5918, 0.6036⟩	⟨0.5818, 0.5937, 0.6056⟩	⟨1.9761, 2.0164, 2.0567⟩	⟨0.0000, 0.0000, 0.0000⟩	⟨0.9800, 1.0000, 1.0200⟩
Huizhou	⟨1.3122, 1.3389, 1.3657⟩	⟨1.0174, 1.0381, 1.0589⟩	⟨0.5557, 0.5671, 0.5784⟩	⟨0.5230, 0.5337, 0.5444⟩	⟨0.9961, 1.0164, 1.0367⟩	⟨0.0000, 0.0000, 0.0000⟩	⟨0.9800, 1.0000, 1.0200⟩
Ningbo	⟨1.2279, 1.2530, 1.2780⟩	⟨1.0662, 1.0880, 1.1097⟩	⟨0.4539, 0.4631, 0.4724⟩	⟨0.5113, 0.5217, 0.5321⟩	⟨2.5223, 2.5738, 2.6252⟩	⟨0.0000, 0.0000, 0.0000⟩	⟨0.9800, 1.0000, 1.0200⟩
Xuzhou	⟨0.8585, 0.8760, 0.8935⟩	⟨1.0056, 1.0262, 1.0467⟩	⟨0.6426, 0.6558, 0.6689⟩	⟨0.6614, 0.6749, 0.6883⟩	⟨1.2692, 1.2951, 1.3210⟩	⟨0.0000, 0.0000, 0.0000⟩	⟨0.9800, 1.0000, 1.0200⟩
Wenzhou	⟨0.9535, 0.9729, 0.9924⟩	⟨1.0609, 1.0825, 1.1042⟩	⟨0.6402, 0.6533, 0.6664⟩	⟨0.5895, 0.6015, 0.6135⟩	⟨8.0970, 8.2623, 8.4275⟩	⟨0.0019, 0.0020, 0.0020⟩	⟨0.9742, 0.9940, 1.0139⟩
Haerbin	⟨0.1297, 0.1324, 0.1350⟩	⟨0.8412, 0.8584, 0.8756⟩	⟨0.6161, 0.6287, 0.6413⟩	⟨0.5753, 0.5871, 0.5988⟩	⟨3.1810, 3.2459, 3.3108⟩	⟨0.0198, 0.0202, 0.0206⟩	⟨0.9305, 0.9495, 0.9685⟩
Zhoukou	⟨1.1169, 1.1397, 1.1625⟩	⟨1.2137, 1.2385, 1.2632⟩	⟨0.5830, 0.5949, 0.6068⟩	⟨0.4818, 0.4916, 0.5015⟩	⟨1.2210, 1.2459, 1.2708⟩	⟨0.0129, 0.0132, 0.0134⟩	⟨0.9671, 0.9868, 1.0066⟩
Zhongshan	⟨1.9580, 1.9980, 2.0380⟩	⟨0.8216, 0.8384, 0.8551⟩	⟨0.6014, 0.6137, 0.6260⟩	⟨0.5838, 0.5958, 0.6077⟩	⟨1.0925, 1.1148, 1.1370⟩	⟨0.0000, 0.0000, 0.0000⟩	⟨0.9224, 0.9412, 0.9600⟩
Qingdao	⟨2.2506, 2.2965, 2.3424⟩	⟨0.9690, 0.9887, 1.0085⟩	⟨0.6575, 0.6709, 0.6843⟩	⟨0.6082, 0.6206, 0.6330⟩	⟨0.9800, 1.0000, 1.0200⟩	⟨0.0161, 0.0164, 0.0167⟩	⟨0.9479, 0.9672, 0.9866⟩
Fuzhou	⟨1.5994, 1.6321, 1.6647⟩	⟨1.1597, 1.1833, 1.2070⟩	⟨0.6727, 0.6864, 0.7001⟩	⟨0.6025, 0.6148, 0.6271⟩	⟨1.1567, 1.1803, 1.2039⟩	⟨0.0136, 0.0139, 0.0142⟩	⟨0.9664, 0.9861, 1.0058⟩
Changzhou	⟨1.8208, 1.8579, 1.8951⟩	⟨1.0204, 1.0412, 1.0621⟩	⟨0.7120, 0.7266, 0.7411⟩	⟨0.5995, 0.6118, 0.6240⟩	⟨0.8193, 0.8361, 0.8528⟩	⟨0.0000, 0.0000, 0.0000⟩	⟨0.9800, 1.0000, 1.0200⟩
Shaoxing	⟨0.9720, 0.9918, 1.0117⟩	⟨1.0411, 1.0623, 1.0836⟩	⟨0.6971, 0.7113, 0.7255⟩	⟨0.5660, 0.5776, 0.5891⟩	⟨0.6748, 0.6885, 0.7023⟩	⟨0.0000, 0.0000, 0.0000⟩	⟨0.9567, 0.9762, 0.9957⟩
Wuhan	⟨1.2702, 1.2961, 1.3221⟩	⟨1.0555, 1.0770, 1.0986⟩	⟨0.3379, 0.3448, 0.3517⟩	⟨0.1611, 0.16430.1676⟩	⟨802.5557, 818.9344, 835.3131⟩	⟨0.0482, 0.0491, 0.0501⟩	⟨0.7383, 0.7534, 0.7685⟩
Nanning	⟨1.6146, 1.6476, 1.6805⟩	⟨1.0735, 1.0954, 1.1173⟩	⟨0.5517, 0.5629, 0.5742⟩	⟨0.5067, 0.5170, 0.5274⟩	⟨0.8836, 0.9016, 0.9197⟩	⟨0.0000, 0.0000, 0.0000⟩	⟨0.9800, 1.0000, 1.0200⟩
Jiaxing	⟨1.5710, 1.6031, 1.6352⟩	⟨1.1141, 1.1368, 1.1596⟩	⟨0.4815, 0.4913, 0.5011⟩	⟨0.4624, 0.4718, 0.4812⟩	⟨0.7230, 0.7377, 0.7525⟩	⟨0.0000, 0.0000, 0.0000⟩	⟨0.9582, 0.9778, 0.9973⟩
Handan	⟨1.7198, 1.7549, 1.7900⟩	⟨1.0008, 1.0212, 1.0416⟩	⟨0.5968, 0.6090, 0.6212⟩	⟨0.6135, 0.6260, 0.6386⟩	⟨0.5141, 0.5246, 0.5351⟩	⟨0.0000, 0.0000, 0.0000⟩	⟨0.9800, 1.0000, 1.0200⟩
Lishui	⟨1.2944, 1.3208, 1.3472⟩	⟨1.0599, 1.0815, 1.1031⟩	⟨0.5433, 0.5544, 0.5655⟩	⟨0.5073, 0.5177, 0.5280⟩	⟨0.4498, 0.4590, 0.4682⟩	⟨0.0000, 0.0000, 0.0000⟩	⟨0.6300, 0.6429, 0.6557⟩
Linyi	⟨1.4639, 1.4938, 1.5236⟩	⟨1.0178, 1.0386, 1.0594⟩	⟨0.4911, 0.5011, 0.5111⟩	⟨0.5103, 0.5207, 0.5311⟩	⟨0.7872, 0.8033, 0.8193⟩	⟨0.0000, 0.0000, 0.0000⟩	⟨0.9800, 1.0000, 1.0200⟩
Weifang	⟨0.7888, 0.8049, 0.8210⟩	⟨0.9565, 0.9760, 0.9955⟩	⟨0.6724, 0.6862, 0.6999⟩	⟨0.5987, 0.6109, 0.6231⟩	⟨0.7069, 0.7213, 0.7357⟩	⟨0.0000, 0.0000, 0.0000⟩	⟨0.9800, 1.0000, 1.0200⟩

CCN: the average confirmed cases number. Among 50INCPM, the average confirmed cases number (CCN) is 2 people per day, except for Wuhan. In many cities, the CCN is low. The CNN in Xiangxi is the smallest; it is 1 people per day. Wuhan is the outbreak center of COVID-19 in 2020 in China, the average CCN is 818 per day while the largest CCN is 1296. So Wuhan is treated as a strange value in the CCN during the process of calculation; it is removed from the evaluation of the average trend, but it is taken into account in the evaluation of the largest CNN. Thus, we use the TFNs $\langle 0, 0, 2 \rangle$, $\langle 0, 2, 4 \rangle$, $\langle 2, 1300, 1300 \rangle$ to express language fuzzy constraints for low, medium and high CCN, respectively see Figure 8.

RR: recovery rate. The average value of the recovery rate (RR) is 0.9574 in 50INCPM. Almost half of 50INCPM has the largest RR. The RR in Lishui is the smallest; it is 0.6429. In addition, it should be mentioned that the RR of Wuhan is the second to last; the RR is 0.7534. Thus, we use the TFNs $\langle 0, 0, 0.9574 \rangle$, $\langle 0.9148, 0.9574, 1 \rangle$ and $\langle 0.9574, 1, 1 \rangle$ to express language fuzzy constraints for low, medium and high RR, respectively; see Figure 9.

MR: mortality rate. The average value of the mortality rate (MR) is 0.0114 in 50INCPM. The MR in Suihua is the largest; it is 0.1538. Wuhan follows Suihua; the MR is 0.0597. The MR in more than half of the cities is 0. Thus, we use the TFNs $\langle 0, 0, 0.0114 \rangle$, $\langle 0, 0.0114, 0.0228 \rangle$ and $\langle 0.0114, 0.2, 0.2 \rangle$ to express the language fuzzy constraints for low, medium and high MR, respectively; see Figure 10.

The urban resilience index (URI) acts as an output variable, and the respective TFNs of URI are formulated as $\langle 0, 0, 0.5 \rangle$, $\langle 0.3, 0.5, 0.7 \rangle$ and $\langle 0.5, 1, 1 \rangle$ to express the language fuzzy constraints as low, medium and high, respectively; see Figure 11.
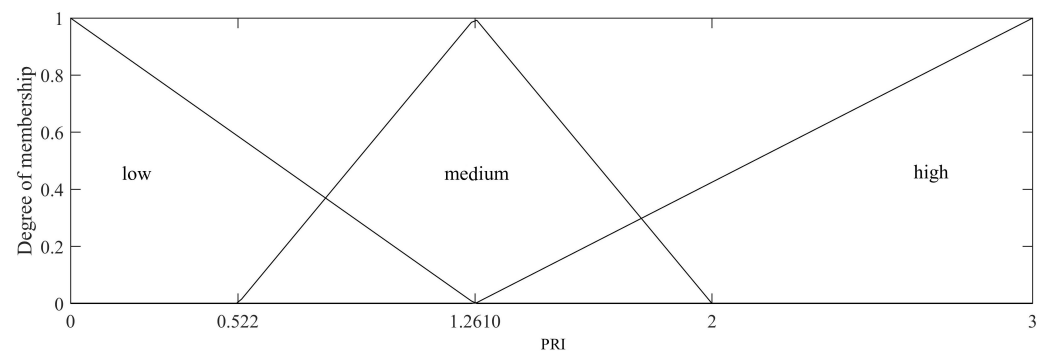
Figure 4. The linguistic hedges of PRI.
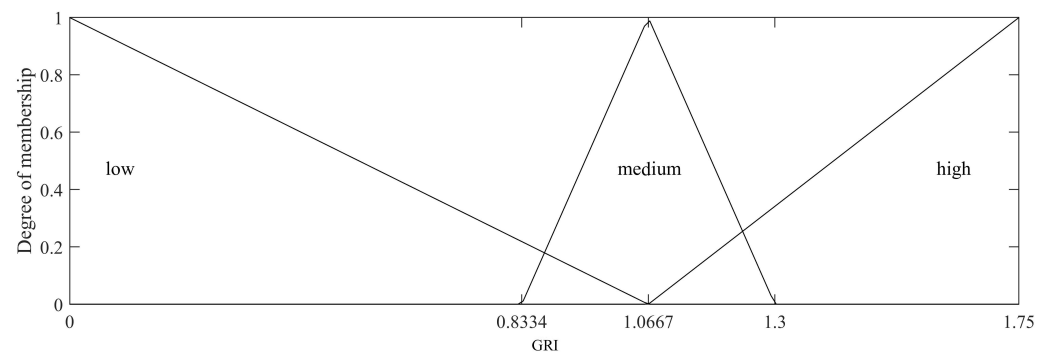
Figure 5. The linguistic hedges of GRI.
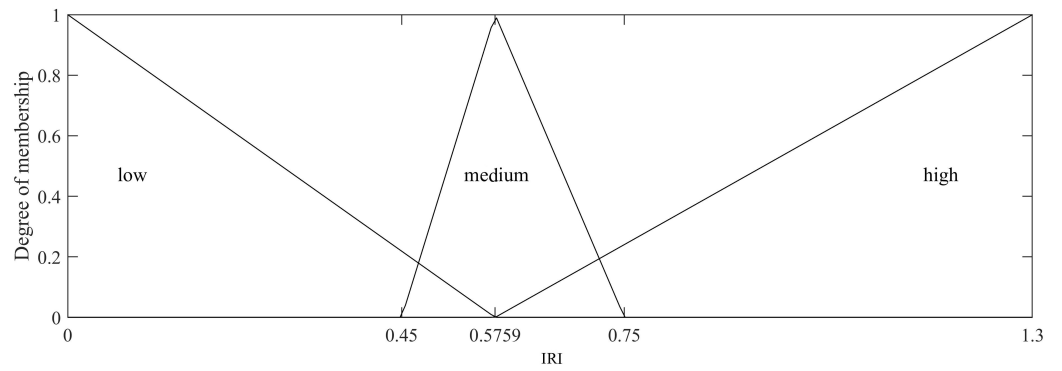
Figure 6. The linguistic hedges of IRI.
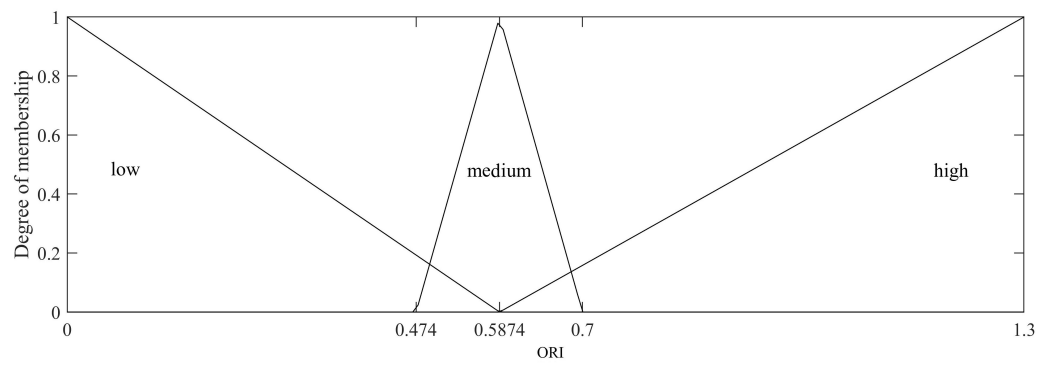
Figure 7. The linguistic hedges of ORI.
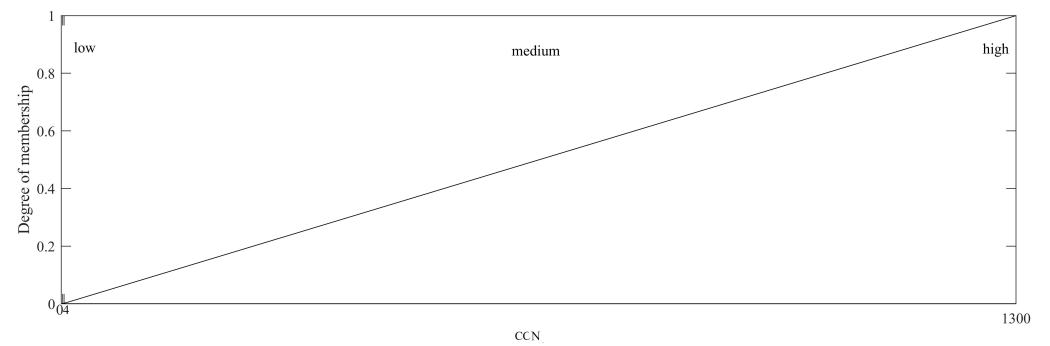
Figure 8. The linguistic hedges of CCN.
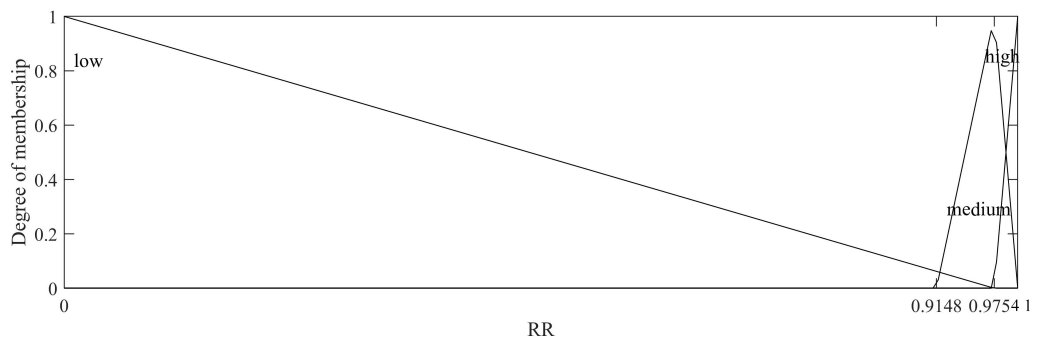
Figure 9. The linguistic hedges of RR.
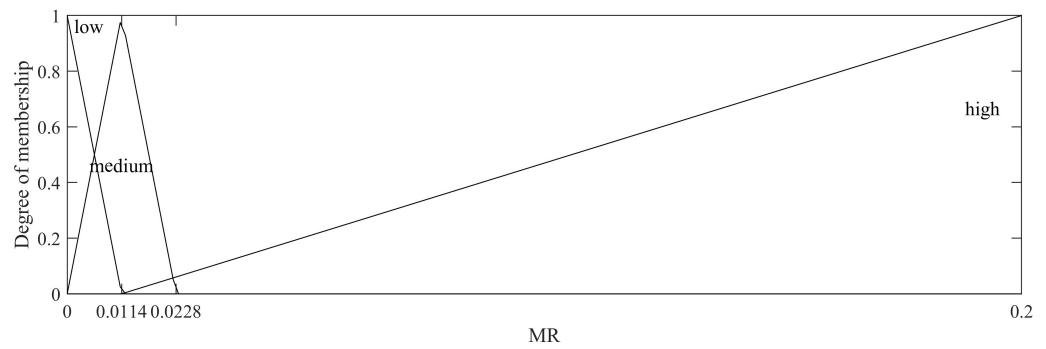
Figure 10. The linguistic hedges of MR.
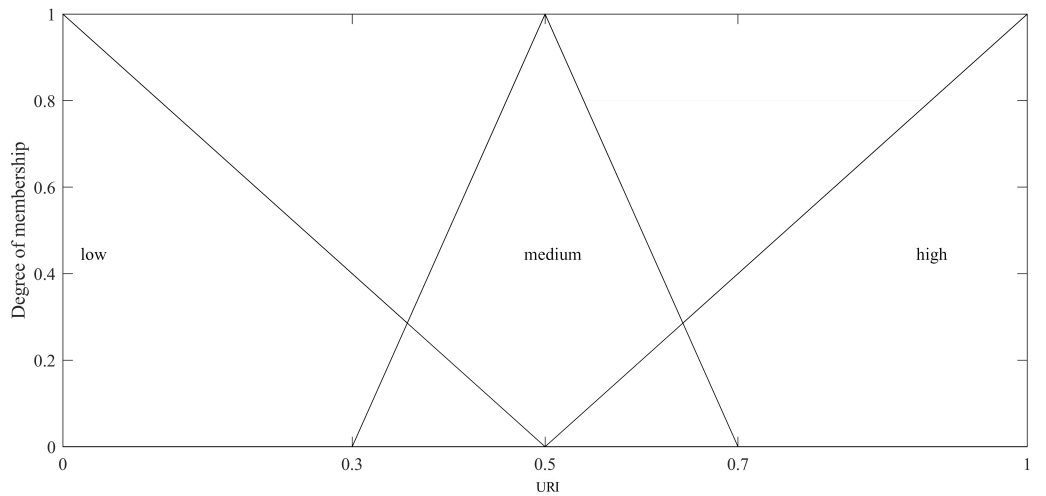
Figure 11. The linguistic hedges of URI.

4.2. Formation of Fuzzy Rule Base

PI, GI, II, OI, CCM, MR, and RR are membership functions for input variables, The urban recovery index (UI) is the membership function for the output variable. The above eight indicators are divided into three levels according to Table 2: high, medium and low. The rules are as follows: If (CCM is low) and (RR is low) and (MR is low) and (PI is low) and (GI is low) and (OI is medium) and (II is low), then (UI is low) format input. Considering that there are many indicators selected in this paper, the weights of each factor are consistent and, except CCM, MR and OI, which are negative influences, the others are positive influences. Therefore, when fuzzy rules are considered, the low, medium and high levels are set to 1, 2 and 3, respectively. Negative effects are set to -3, -2, -1, and combined addition operations are performed on each level of the seven factors to obtain 2187 rules with the range $[-1, 13]$. The value range is $[-1, 3]$, the UI value is 1, and there are 274 items; the value field is $[4, 8]$, the UI value is 2, and there are 1639 items; and the value field is $[9, 13]$, the UI value is 3, and there are 274 items. We establish the following rule matrix:

$$
\begin{bmatrix}
1 & 1 & -3 & 1 & 1 & -3 & 1 & 1 & 1 & 1 \\
2 & 2 & -3 & 1 & 3 & -2 & 3 & 2 & 1 & 1 \\
2 & 3 & -3 & 2 & 1 & -2 & 2 & 2 & 1 & 1 \\
2 & 2 & -2 & 3 & 3 & -2 & 3 & 3 & 1 & 1 \\
3 & 3 & -2 & 3 & 1 & -3 & 1 & 2 & 1 & 1 \\
\cdots & \cdots & \cdots & \cdots & \cdots & \cdots & \cdots & \cdots & \cdots & \cdots
\end{bmatrix}
\tag{7}
$$

where the second-to-last element of each row in the matrix, 1, represents the weight, and the last element represents the logical relationship between the various factors. "and" is a

1, "or" is a 2. To facilitate the calculation, a bias of about 2% of the collected data is taken into account when deriving TFN as the input.

Table 2. The inference rules of variables.

Rules	If							Then
	CCN	RR	MR	PRI	GRI	ORI	IRI	URI
1	low	low	low	low	low	low	low	low
2	low	low	low	low	low	low	medium	low
3	low	low	low	low	low	low	high	low
⋮	⋮	⋮	⋮	⋮	⋮	⋮	⋮	⋮
26	low	low	low	low	high	high	medium	medium
27	low	low	low	low	high	high	high	medium
28	low	low	low	medium	low	low	low	low
⋮	⋮	⋮	⋮	⋮	⋮	⋮	⋮	⋮
1198	medium	medium	high	high	medium	low	low	medium
1199	medium	medium	high	high	medium	low	medium	medium
1200	medium	medium	high	high	medium	low	high	medium
⋮	⋮	⋮	⋮	⋮	⋮	⋮	⋮	⋮
2185	high	high	high	high	high	high	low	high
2186	high	high	high	high	high	high	medium	high
2187	high	high	high	high	high	high	high	high

Since every input and output variable consists of three linguistic terms, the CCN, MR and ORI are negative variables, while PRI, GRI, IRI and RR are positive variables in the operation. When the fuzzy rules are written on Matlab software(2018b), the low, medium and high positive indicators are set as 1, 2 and 3, and the low, medium and high negative variables are set as −3, −2 and −1. The rule base of the proposed MFIS contains a total number of $3^7 = 2187$ "if–then" fuzzy rules, which are presented in Table 2.

By combining all the possible outcomes corresponding to the input and output variables, the value domain is equally divided. The URI is low when the value domain is [−1, 3], and there are 274 "if–then" fuzzy rules in this range. The URI is medium when the value domain is [4, 8]; there are 1639 "if–then" fuzzy rules in this range. The URI is high when the value domain is [9, 13]; there are 274 "if–then" fuzzy rules in this range. Through the aggregation and defuzzification of the obtained results, the corresponding value of the URI in each city is obtained.

5. URI of the 50 Important Node Cities under the Influence of COVID-19

5.1. The Spacial Distribution of URI of the 50 Important Node Cities

The URI of 50INCPM decreases from the eastern coastal area to the western inland under the influence of COVID-19. The cities with a URI of more than 0.5 gather in Guangdong, Zhejiang, Jiangsu and Shandong provinces of China. The URI of the cities in central China is generally low. The average URI of 50INCPM under the influence of COVID-19 is 0.5119. The URI in Qingyuan is the largest; it is 0.6855. The URI in Shaoxing is the smallest; it is 0.3303. See Table 3.

As COVID-19 is controlled, the URI is gradually rising. The growth rate of the URI of southeast coastal cities exceeds that of inland cities; this trend is consistent with the existing research results [51]. Furthermore, the impact of COVID-19 on first-tier cities is higher than that in second-tier and third-tier cities. From the overall evaluation results, the top 10 cities ranked by URI are Qingyuan, Heze, Xiangxi, Changzhou, Handan, Ningbo, Linyi, Qingdao, Wuxi and Huizhou, but none of the first-tier cities in inland China (Beijing, Shanghai, Guangzhou and Shenzhen) are ranked in the top 10 cities of URI. So, in the case of large-scale emergencies, neither metropolises nor small cities have the highest resilience, as second-tier and third-tier cities have stronger resilience, especially the second- and third-tier cities along the eastern seaboard.

Due to the COVID-19 pandemic, the economy and living in first-tier cities have been greatly affected; the URI of Shanghai and Guangzhou both are only 0.5, and the URI of Beijing is lower than 0.5. It is necessary to take a look at Wuhan, where the URI is

only 0.3511 (Figure 12). Wuhan is the epicenter of COVID-19 in China, and thus the transportation, economy and everyday life have all been hit the hardest [52]. The daily CCN and MR are staggering. Thus, the GOC has adopted the strictest prevention and control policy in Wuhan; it is under lockdown. All residents of Wuhan are not allowed to leave Wuhan, and people from other places are not allowed to visit Wuhan [52]. In addition, necessary community places, such as farmers markets, shopping malls and supermarkets, are closed, and services such as hotels and guesthouses are also prohibited. As a matter of fact, although residents are uncomfortable with such strict controls, it seemed to be the best way to contain the spread of COVID-19 at the time. Internationally, maximal barrier approaches are also adopted by most other countries in Western Europe [5]. The exception is that Sweden's strategy to manage the spread of COVID-19 has not included any form of lockdown, but the COVID-19 pandemic has brought changes for society, significantly disrupting everyday life, during a relatively short period of time [53].
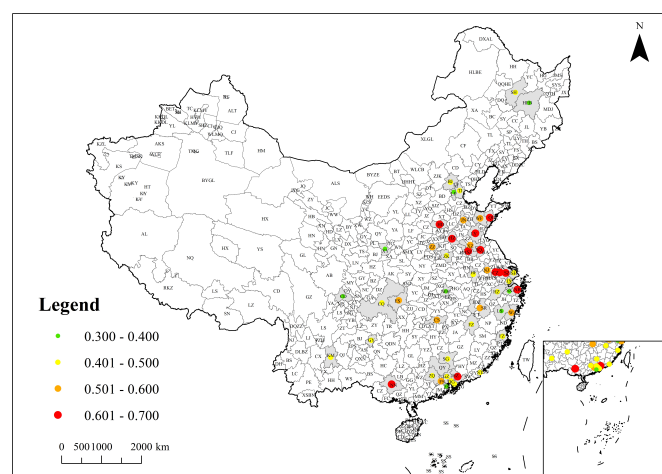
Figure 12. URI of the selected 50 important node cities.

5.2. The URI of the 50 Important Node Cities in Each Period

(1) In the incubative period, from 15 January to 31 January 2020, the average URI of 50INCPM is 0.3816. The URI in Heze is the largest; it is 0.6695. The URI in Shaoxing is the smallest; it is 0.3161. Affected by COVID-19, the URI of Guangzhou is lower relatively, just 0.3175. It is only higher than that of Shaoxing; see Figure 13. Compared with the western cities, the eastern cities have a higher URI, cities with higher URI are all located in the eastern coastal area, which shows agglomeration characteristics in space; they are Heze, Handan, Shanghai, Suzhou, Ningbo and Zhaoqing. For western cities of China, except for Xi 'an, Xianyang, Chongqing and Chengdu, the rest of the western cities have lower URI, and they are relatively scattered in space.

(2) During the pandemic period, from 1 February 2020 to 20 February 2020, the most serious stage of COVID-19, the URI is generally lower in each city. The average URI of 50INCPM is 0.3263. The URI in Enshi is the largest; it is 0.3511. The URI in Jinan is the smallest; it is 0.2928. In addition, the URI of Wuhan is relatively low; it is only 0.3144. See Figure 13. The calculation results in the pandemic period show that the impact of COVID-19 on cities in mainland China is very widespread. Cities with higher URI are distributed in the eastern coastal zone, showing agglomeration characteristics, higher URI concentrated in Beijing, Heze, Shanghai, Ningbo and Zhaoqing. For western cities of China, except for Xianyang, Xi'an, Chengdu, Chongqing and Kunming, the URIs of western cities are generally lower and more dispersed. Compared to the incubative period, the URIs in this period showed the Matthew effect, in which eastern developed cities are more resilient and western cities are more vulnerable. At the same time, the URI presents a cluster distribution. In other words, the cities with high

URIs are clustered together and the cities with low URIs are focused together, which makes for obvious differences between the east and the west cities.

(3) In the controlled period, from 21 February 2020 to 15 March 2020, the average URI of 50INCPM is 0.5138, the URI in Xiangxi is the largest, at 0.6879, and the URI in Xianyang is the smallest, at 0.3257. It is worth noting that the URI in Wuhan is still low. It is just 0.3511; see Figure 13. During the controlled period, the URI of all cities is increased, but the trend in cities along the southeast coast is more obvious, and it is concentrated in Qingdao, Heze, Suzhou, Ningbo, Shantou, and Qingyuan. This increasing trend has obvious regional agglomeration.

Table 3. The rank of the selected top 50 important node cities in the selected three stages and the total URI.

City	URI-I	City	URI-II	City	URI-III	City	URI	Rank
Heze	0.6695	Enshi	0.3511	Xiangxi	0.6879	Qingyuan	0.6855	1
Suihua	0.5161	Linyi	0.3425	Ningbo	0.6798	Heze	0.6695	2
Chongqing	0.5000	Xiangxi	0.3423	Nanning	0.6764	Xiangxi	0.6561	3
Shantou	0.5000	Lishui	0.3397	Heze	0.6695	Changzhou	0.6533	4
Zhoukou	0.4944	Shantou	0.3384	Kunming	0.6671	Handan	0.6398	5
Handan	0.4826	Harbin	0.3378	Qingyuan	0.6650	Ningbo	0.6387	6
Nanning	0.4667	Heze	0.3374	Shantou	0.6625	Linyi	0.6373	7
Linyi	0.4255	Zhongshan	0.3368	Wuxi	0.6583	Qingdao	0.6346	8
Dongguan	0.4246	Qingyuan	0.3360	Changzhou	0.6533	Wuxi	0.6322	9
Fuzhou	0.4133	Zhoukou	0.3344	Linyi	0.6464	Huizhou	0.6293	10
Changzhou	0.4130	Langfang	0.3335	Foshan	0.6435	Nanning	0.6257	11
Zhaoqing	0.4077	Xuzhou	0.3333	Guiyang	0.6378	Suzhou	0.6195	12
Qingyuan	0.4045	Tianjin	0.3328	Huizhou	0.6333	Suqian	0.6063	13
Shanghai	0.3954	Guiyang	0.3324	Zhongshan	0.6277	Foshan	0.5932	14
Hefei	0.3935	Zhengzhou	0.3315	Qingdao	0.6260	Wenzhou	0.5872	15
Guiyang	0.3912	Hangzhou	0.3313	Suzhou	0.6208	Jinan	0.5719	16
Kunming	0.3888	Handan	0.3310	Suqian	0.6174	Nanjing	0.5685	17
Zhengzhou	0.3879	Ningbo	0.3306	Shangrao	0.6158	Zhengzhou	0.5454	18
Beijing	0.3871	Changzhou	0.3305	Wenzhou	0.5917	Changsha	0.5433	19
Foshan	0.3778	Huizhou	0.3290	Hefei	0.5660	Shangrao	0.5319	20
Enshi	0.3707	Weifang	0.3284	Zhoukou	0.5567	Enshi	0.5173	21
Jiaxing	0.3680	Shanghai	0.3281	Chongqing	0.5304	Xuzhou	0.5151	22
Wenzhou	0.3641	Shenzhen	0.3281	Changsha	0.5233	Weifang	0.5062	23
Huizhou	0.3636	Xianyang	0.3277	Jiaxing	0.5127	Zhaoqing	0.5000	24
Jinan	0.3626	Dongguan	0.3274	Xuzhou	0.5115	Shanghai	0.5000	25
Qingdao	0.3597	Qingdao	0.3261	Weifang	0.5062	Suihua	0.5000	26
Zhongshan	0.3589	Shangrao	0.3254	Shenzhen	0.5000	Guangzhou	0.5000	27
Wuxi	0.3581	Suqian	0.3251	Zhengzhou	0.5000	Hefei	0.5000	28
Suqian	0.3542	Hefei	0.3251	Handan	0.5000	Guiyang	0.5000	29
Hangzhou	0.3512	Kunming	0.3248	Zhaoqing	0.5000	Shenzhen	0.5000	30
Lishui	0.3475	Chongqing	0.3245	Hangzhou	0.4878	Zhoukou	0.5000	31
Wuhan	0.3445	Changsha	0.3239	Fuzhou	0.4775	Chongqing	0.5000	32
Chengdu	0.3416	Fuzhou	0.3234	Nanjing	0.4623	Jiaxing	0.4951	33
Shaoguan	0.3382	Nanjing	0.3233	Chengdu	0.4599	Kunming	0.4941	34
Harbin	0.3378	Shaoguan	0.3231	Dongguan	0.4461	Hangzhou	0.4878	35
Weifang	0.3377	Chengdu	0.3229	Jinan	0.4308	Fuzhou	0.4800	36
Xianyang	0.3353	Wenzhou	0.3224	Guangzhou	0.4236	Shantou	0.4598	37
Suzhou	0.3348	Guangzhou	0.3212	Enshi	0.3824	Beijing	0.4276	38
Shenzhen	0.3342	Zhaoqing	0.3203	Shaoguan	0.3680	Shaoguan	0.4096	39
Xuzhou	0.3333	Xian	0.3202	Shaoxing	0.3649	Dongguan	0.4081	40
Tianjin	0.3328	Beijing	0.3200	Lishui	0.3538	Tianjin	0.4045	41
Nanjing	0.3322	Suzhou	0.3199	Wuhan	0.3511	Xian	0.3987	42
Langfang	0.3311	Suihua	0.3193	Xian	0.3442	Chengdu	0.3734	43
Shangrao	0.3271	Foshan	0.3192	Shanghai	0.3439	Xianyang	0.3720	44
Xiangxi	0.3222	Wuhan	0.3144	Suihua	0.3421	Zhongshan	0.3650	45
Changsha	0.3217	Wuxi	0.3095	Beijing	0.3384	Harbin	0.3554	46
Ningbo	0.3212	Nanning	0.3094	Harbin	0.3378	Wuhan	0.3512	47
Xian	0.3202	Shaoxing	0.3071	Tianjin	0.3328	Lishui	0.3455	48
Guangzhou	0.3175	Jiaxing	0.3019	Langfang	0.3311	Langfang	0.3311	49
Shaoxing	0.3161	Jinan	0.2928	Xianyang	0.3257	Shaoxing	0.3303	50

Comprehensively, it is not difficult to see that the impact of COVID-19 on Chinese mainland cities is very common and obvious. The URIs in the eastern coastal cities are

higher than those in western cities. From the point of regional distribution, eastern cities with higher URI are gathered; they form a cluster pattern of distribution. It is interesting to note that cities with the biggest URI are not first-tier cities, but the second-tier and third-tier cities have stronger resilience in the case of large-scale emergencies. At the same time, the Matthew effect of urban URI is more obvious when an extreme event appears.

(**a**)   (**b**)

(**c**)
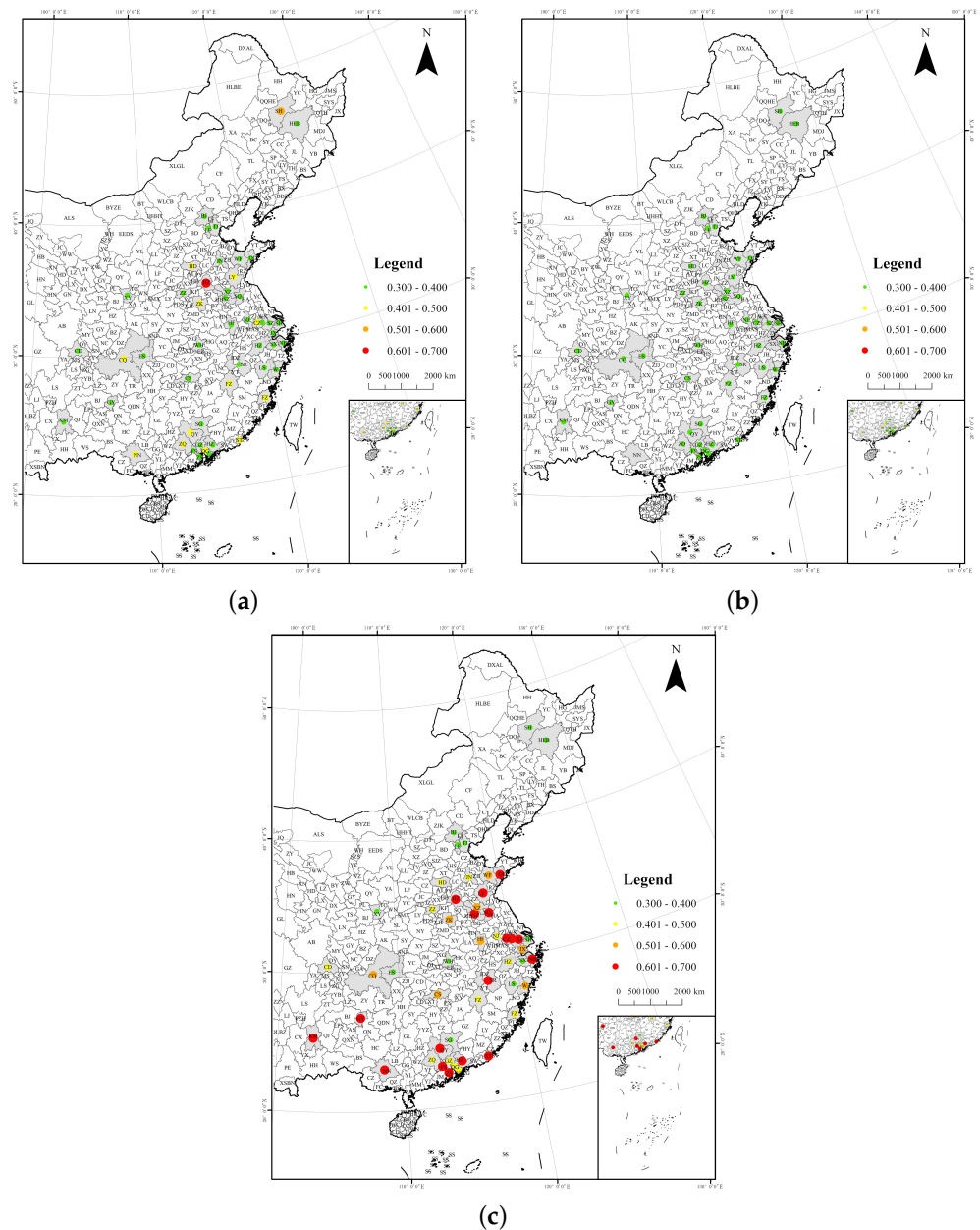
Figure 13. URI in the 50 important node cities of each period. (**a**) The incubative period; (**b**) the pandemic period; (**c**) the controlled period.

5.3. The Correlation between URI and RR

On the whole, the URI varies between 0.4 and 0.6 and the RR in each city is from 0.8 to 1; see Figure 14. In the incubative period, the URI is about 0.4, and the RR is extremely low because this is the beginning of COVID-19 and residents have not taken it seriously enough; see Figure 15. In the pandemic period, the URI is steady around 0.4, and the RR increases rapidly in each city; see Figure 16. In the controlled period, the URI varies between 0.4 and 0.6, and the RR in each city is about to reach 1; see Figure 17.

In this subsection, we give the correlation of URI and RR. The correlation analysis shows that the correlation of URI and RR is 0.549, and the *p* value is 0.000 with a significant effect at the 1% level. That is to say, there exists a positive correlation in URI and RR, and the details are illustrated in Figures 14–17.
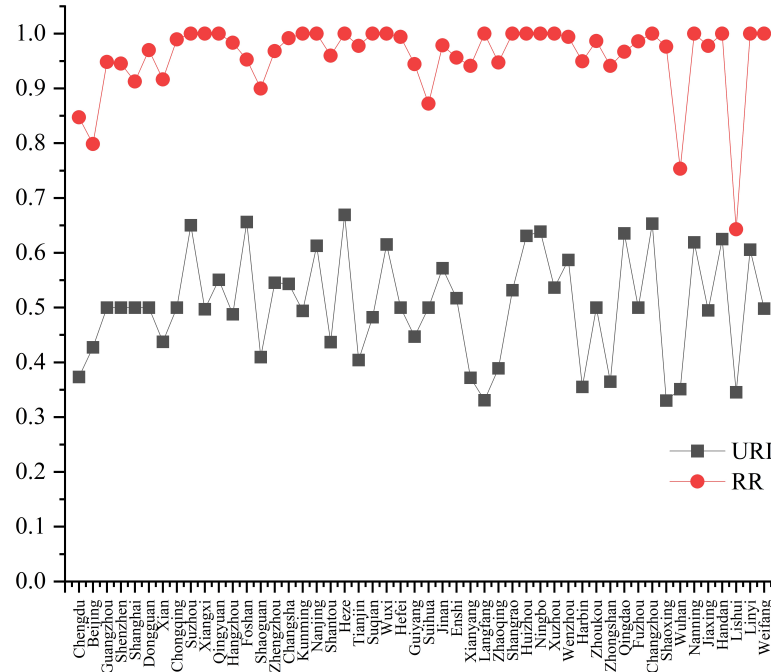
Figure 14. The correlation between URI and RR.
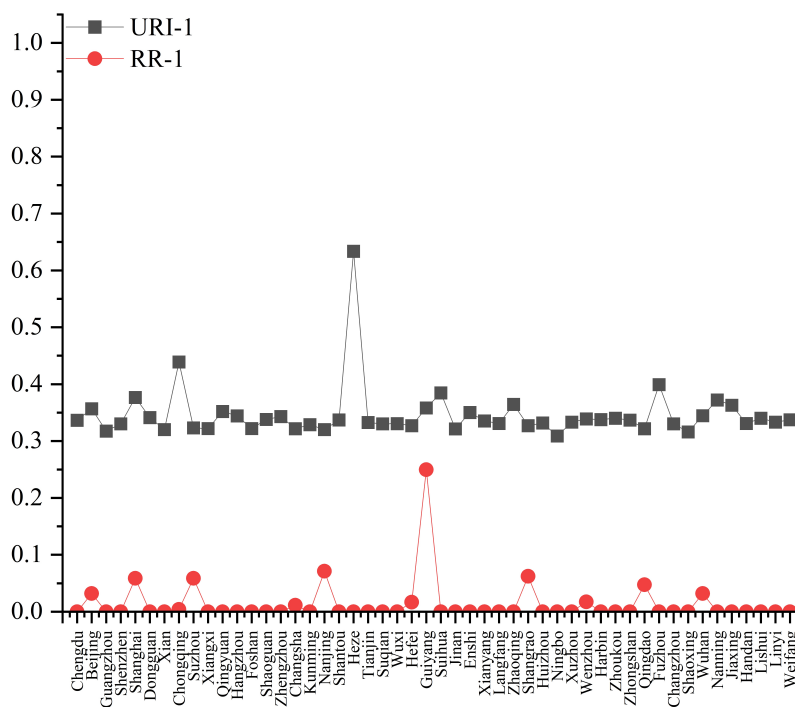
Figure 15. The correlation between URI and RR during the incubative period.
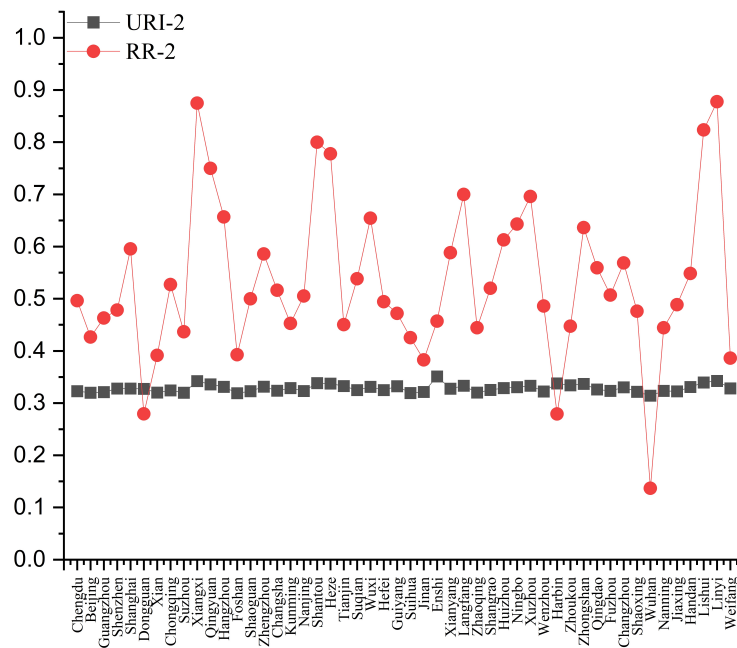
Figure 16. The correlation between URI and RR during the pandemic period.
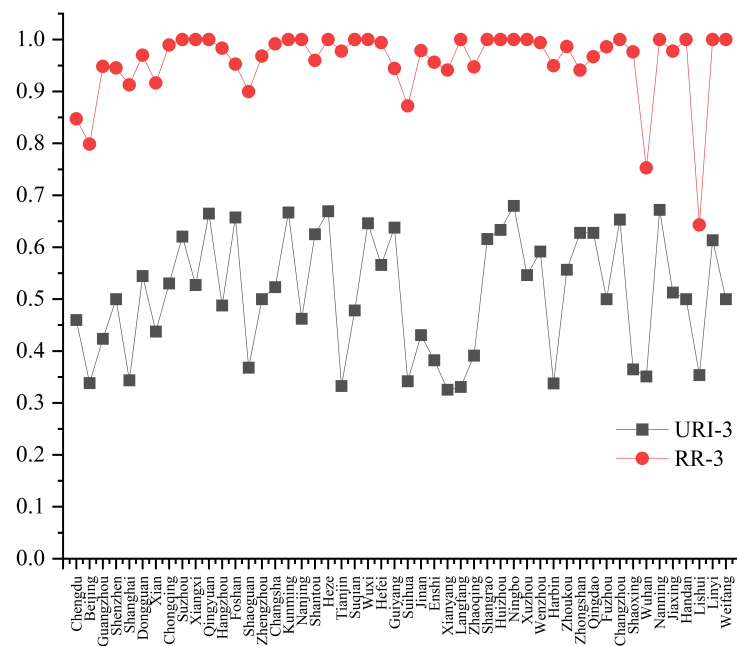
Figure 17. The correlation between URI and RR during the controlled period.

6. Discussion and Conclusions

6.1. Discussion

In most existing studies, the proposed methods on the impact of COVID-19 are mostly qualitative analyses and simple comprehensive weighting methods. To some extent, the qualitative analysis can clarify the impact of COVID-19, but it cannot clearly calculate the impact degree of COVID-19. As for the simple comprehensive weighting method, which relies heavily on the experience of experts. So, it is subjective. However, the MFIS proposed in this article on the basis of fuzzy logic can obtain urban resilience under the influence of COVID-19 from the information derived from data itself through FIS.

In reality, errors of data are unavoidable, as statistical negligence along with statistical path inconsistency and fuzzification can handle these problems of data well. Therefore, via fuzzification, all crisp inputs as TFNs, this article can extract the information contained in the data as much as possible so that the results obtained can more objectively reflect the urban resilience under the influence of COVID-19.

Beyond these, it should be pointed out that the infrastructure, such as hospitals, airports, railway stations and the number of vaccine injections in a city cannot be ignored when evaluating urban resilience under the influence of the COVID-19 pandemic. However, because relevant effective indicators cannot be obtained, these indicators are not considered in this paper. Therefore, in the later research, we will refine indicators to improve our research from a more comprehensive perspective.

Finally, we hope that the research in this article can provide reference for local governments to formulate urban restoration measures under COVID-19 and contribute to defeating COVID-19 in Chinese cities and even global cities.

6.2. Conclusions

The COVID-19 pandemic has harmed people's mental and physical health and produced unhealthy psychological emotions, such as stress and discrimination. Meanwhile, building an urban resilience assessment framework and comprehensive assessment of urban resilience building status and development can make up for the shortcomings of the city. So, it is necessary to assess the urban resilience of cities. We select the population inflow and outflow data in 2019 and 2020 to reflect the population migration in important node cities in population migration. We apply MFIS in approximating the urban resilience index (URI) based on multiple inputs. Therefore, in order to calculate the URI of cities, we use the PRI and GRI to reflect the impact of the COVID-19 pandemic on society and economy, IRI and ORI to characterize the changes in population mobility under the COVID-19 pandemic, and CCN, RR, and MR of COVID-19 to show the situation of the COVID-19 pandemic in this paper. And we explore a new approach based on the MFIS model. Meanwhile, based on the big data of population migration and COVID-19 data in China from 15 January to 15 March in 2020, we calculate the URI of 50INCPM in China in 2020 under the influence of the COVID-19 pandemic. Moreover, we show the spatial difference of URI and its changes in different stages in order to solve the following problems. (i) How is the resilience of 50INCPM in China in 2020 under the influence of the COVID-19 pandemic? (ii) In the case of large-scale emergencies, which has stronger resilience, metropolises or small cities? The obtained results show the following:

(i)　Under the influence of the COVID-19 pandemic, most of 50INCPM in 2020 is concentrated along the southeast coast of China. The URI of 50INCPM decreases from the eastern coastal area to the western inland, the cities with a URI greater than 0.5 are gathered in Guangdong, Zhejiang, Jiangsu and Shandong provinces. As the COVID-19 pandemic is being controlled, the URI is gradually rising. The growth rate of URI in southeast coastal cities exceeds that of inland cities. So, it can be seen that the impact of the COVID-19 pandemic on inland cities is higher than that on coastal cities.

(ii)　The second-tier and third-tier cities have stronger resilience in the case of large-scale emergencies.

(iii)　There exists a positive correlation in URI and RR. The correlation analysis shows that the correlation of URI and RR is 0.549, and the *p* value is 0.000 with a significant effect at the 1% level.

Broadly speaking, as can be seen from the results obtained in this paper, the URI of 50INCPM in China is about 0.5. Thus, on the basis of universal vaccine coverage, we hold that the GOC should promote the cities' resilience in China, especially in the first-tier city in inland China (Beijing, Shanghai, Guangzhou and Shenzhen) because they are important metropolises regarding the country's political, economic and other social activities, which have leading roles, radiate the driving ability for other cities, and play an important role in leading the country's economic and social development. On the other hand, on the

premise of implementing epidemic prevention and control measures, local governments should stimulate the resilience of each city in terms of population and economy. More precisely, in terms of population, local governments should take improving measures to encourage college students and migrant workers to stay in the city, such as relaxing policies on household registration and employment, and expanding the coverage of government-subsidized housing. In terms of economy, the local governments have to restore the normal production and operation of various markets and entities as soon as possible and in an orderly manner. As for industries that have suffered heavy losses due to the COVID-19 pandemic, the government should reduce taxes as appropriate. As far as residents are concerned, in the consideration of COVID-19 being quite infectious, it is very effective to get vaccinated against COVID-19 or to add a third one, as possible.

References

1. Chen, N.; Zhou, M.; Dong, X.; Qu, J.; Gong, F.; Han, Y.; Qiu, Y.; Wang, J.; Liu, Y.; Wei, Y.; et al. Epidemiological and clinical characteristics of 99 cases of 2019 novel coronavirus pneumonia in Wuhan, China: A descriptive study. *Lancet* **2020**, *395*, 391–393. [CrossRef] [PubMed]
2. Jain, V.; Yuan, J.M. Predictive symptoms and comorbidities for severe COVID-19 and intensive care unit admission: A systematic review and meta-analysis. *Int. J. Public Health* **2020**, *65*, 533–546. [CrossRef] [PubMed]
3. Song, C.Y.; Xu, J.; He, J.Q.; Lu, Y.Q. Immune dysfunction following COVID-19, especially in severe patients. *Sci. Rep.* **2020**, *10*, 15838. [CrossRef] [PubMed]
4. Sohrabi, C.; Alsafi, Z.; O'neill, N.; Khan, M.; Kerwan, A.; Al-Jabir, A.; Agha, R.C. World Health Organization declares global emergency: A review of the 2019 novel coronavirus (COVID-19). *Int. J. Surg.* **2020**, *76*, 71–76. [CrossRef] [PubMed]
5. Narlikar, A.; Sottilotta, C.E. Pandemic narratives and policy responses: West European governments and COVID-19. *J. Eur. Public Policy* **2021**, *28*, 1–20. [CrossRef]
6. Lai, S.; Ruktanonchai, N.W.; Zhou, L.; Prosper, O.; Luo, W.; Floyd, J.R.; Tatem, A.J. Effect of non-pharmaceutical interventions to contain COVID-19 in China. *Nature* **2020**, *585*, 410–413. [CrossRef]
7. Ayalon, L. There is nothing new under the sun: Aageism and intergenerational tension in the age of the COVID-19 outbreak. *Int. Psychogeriatr.* **2020**, *32*, 1221–1224. [CrossRef] [PubMed]
8. Demirba, D.; Bozkurt, V.; Yorun, S. *The COVID-19 Pandemic and Its Economic, Social, and Political Impacts*; Istanbul University Press: Instanbul, Turkey, 2020.
9. Simons, G. A critical review of mass media and non-academic reports forecasts of the economic effects of COVID-19 within the frame of crisis management. *Stud. Russ. Econ. Dev.* **2021**, *32*, 351–356. [CrossRef]
10. Akhtar, N. COVID-19: A great challenge for the tourism industry. *J. Biomed. Pharm. Res.* **2021**, *10*, 83–87. [CrossRef]
11. Wu, F.; Liu, G.; Guo, N.; Li, Z.; Deng, X. The impact of COVID-19 on China's regional economies and industries. *J. Geogr. Sci.* **2021**, *31*, 565–583. [CrossRef]
12. Long, H.; Zhao, J.Z. The impact of SARS epidemic and financial crisis on China's economy structure referenced to the potential impact of COVID-19. *Bull. Appl. Econ.* **2021**, *8*, 97–108. [CrossRef]
13. Roxana, I. Capital market correlations structure during the COVID-19 crisis. *Ann. Econ.* **2020**, *6*, 67–79.
14. Chen, M.; Li, Y.; Chen, J.; Wen, Z.; Feng, F.; Zou, H.; Sun, C. An online survey of the attitude and willingness of Chinese adults to receive COVID-19 vaccination. *Hum. Vaccines Immunother.* **2021**, *17*, 2279–2288. [CrossRef] [PubMed]

15. Sims, A.C.; Burkett, S.E.; Yount, B.; Pickles, R.J. SARS-CoV replication and pathogenesis in an in vitro model of the human conducting airway epithelium. *Virus Res.* **2008**, *133*, 33–44. [CrossRef] [PubMed]

16. Ahadu, E. Novel Corona virus COVID-19: Impact on economic development and mitigating solution for developing countries. *J. Humanit. Soc. Sci.* **2020**, *8*, 86–91. [CrossRef]

17. Adkins, J.K.; Linville, D.; Clarence, B.; Elliott, S.; Paddock, S. The impact of COVID-19 on industry and education. *J. Comput. Sci. Coll.* **2021**, *36*, 80–81.

18. Fu, X.L.; Zhang, J.; Wang, L.M. Introduction to the special section: The impact of COVID-19 and post-pandemic recovery: China and the world economy. *J. Chin. Econ. Bus. Stud.* **2020**, *18*, 311–319. [CrossRef]

19. Sharifi, A.; Yamagata, Y. A conceptual framework for assessment of urban energy resilience. *Energy Procedia* **2015**, *75*, 2904–2909. [CrossRef]

20. Cui, Z.; Fu, X.; Wang, J.; Qiang, Y.; Jiang, Y.; Long, Z. How does COVID-19 pandemic impact cities' logistics performance? An evidence from China's highway freight transport. *Transp. Policy* **2022**, *120*, 11–22. [CrossRef]

21. Zhen, C.; Cheng, M.; Song, M. What determines urban resilience against COVID-19: City size or governance capacity? *Sustain. Cities Soc.* **2021**, *75*, 103304.

22. Khavarian-Garmsir, A.R.; Sharifi, A.; Moradpour, N. Are high-density districts more vulnerable to the COVID-19 pandemic? *Sustain. Cities Soc.* **2021**, *70*, 102911. [CrossRef] [PubMed]

23. Adhikari, S.; Pantaleo, N.P.; Feldman, J.M.; Ogedegbe, O.; Thorpe, L.; Troxel, A.B. Assessment of community-level disparities in coronavirus disease 2019 (COVID-19) infections and deaths in large US metropolitan areas. *JAMA Netw. Open* **2020**, *3*, e2016938. [CrossRef] [PubMed]

24. Valjarević, A.; Milić, M.; Valjarević, D.; Stanojević-Ristić, Z.; Petrović, L.; Milanović, M.; Filipović, D.; Ristanović, B.; Basarin, B.; Lukić, T. Modelling and mapping of the COVID-19 trajectory and pandemic paths at global scale: A geographer's perspective. *Open Geosci.* **2020**, *12*, 1603–1616. [CrossRef]

25. Chen, X.; Quan, R. A spatiotemporal analysis of urban resilience to the COVID-19 pandemic in the Yangtze River Delta. *Nat. Hazards* **2021**, *106*, 829–854. [CrossRef]

26. Hou, X.; Ma, Q.; Wang, X. Spatial differentiation and elements influencing urban resilience in the middle reaches of the Yangtze River under the COVID-19 pandemic. *Discret. Dyn. Nat. Soc.* **2021**, *2021*, 6687869. [CrossRef]

27. Wu, X.; Mao, R.; Guo, X. Equilibrium of Tiered Healthcare Resources during the COVID-19 Pandemic in China: A Case Study of Taiyuan, Shanxi Province. *Int. J. Environ. Res. Public Health* **2022**, *19*, 7035. [CrossRef]

28. Trencher, G.; Broto, V.C.; Takagi, T.; Sprigings, Z.; Nishida, Y.; Yarime, M. Innovative policy practices to advance building energy efciency and retroftting: Approaches, impacts and challenges in ten C40 cities. *Environ. Sci. Policy* **2016**, *66*, 353–365. [CrossRef]

29. Liu, Y. Measurement of urban resilience system development: Based on an empirical study of 288 cities in China. *Urban Dev. Res.* **2021**, *28*, 93–100.

30. Álvarez-Pomar, L.; Rojas-Galeano, S. Impact of personal protection habits on the spread of pandemics: Insights from an agent-based model. *Sci. World J.* **2021**, *1*, 1–14. [CrossRef]

31. Mamdani, E.H.; Assilian, S. An experiment in linguistic synthesis with a fuzzy logic controller. *Int. J. Hum.-Comput. Stud.* **1975**, *7*, 1–13. [CrossRef]

32. Ghosh, B.; Biswas, A. Status evaluation of provinces affected by COVID-19: A qualitative assessment using fuzzy system. *Appl. Soft Comput.* **2021**, *109*, 107540. [CrossRef] [PubMed]

33. Togacar, M.; Ergen, B.; Comert, Z.Z. COVID-19 detection using deep learning models to exploit social mimic optimization and structured chest X-ray images using fuzzy color and stacking approaches. *Comput. Biol. Med.* **2020**, *121*, 103805. [CrossRef] [PubMed]

34. Govindan, K.; Mina, H.; Alavi, B. A decision support system for demand management in healthcare supply chains considering the epidemic outbreaks:A case study of coronavirus disease 2019 (COVID-19). *Transp. Res. Part E Logist. Transp. Rev.* **2020**, *138*, 101967. [CrossRef] [PubMed]

35. Mardani, A.; Saraji, M.K.; Mishra, A.R.; Rani, P. A novel extended approach under hesitant fuzzy sets to design a framework for assessing the key challenges of digital health interventions adoption during the COVID-19 outbreak. *Appl. Soft Comput.* **2020**, *96*, 106613. [CrossRef] [PubMed]

36. Mahmoudi, M.R.; Baleanu, D.; Mansor, Z.; Tuan, B.A.; Pho, K.H. Fuzzy clustering method to compare the spread rate of COVID-19 in the high risks countries. *Chaos Solitons Fractals* **2020**, *140*, 110230. [CrossRef] [PubMed]

37. Behnood, A.; Golafshani, E.M.; Hosseini, S.M. Determinants of the infection rate of the COVID-19 in the U.S. using ANFIS and virus optimization algorithm (VOA). *Chaos Solitons Fractals* **2020**, *139*, 110051. [CrossRef] [PubMed]

38. Ly, K.T. A COVID-19 forecasting system using adaptive neuro-fuzzy inference. *Financ. Res. Lett.* **2021**, *41*, 101844. [CrossRef] [PubMed]

39. Ocampo, L.; Yamagishi, K. Modeling the lockdown relaxation protocols of the philippine government in response to the COVID-19 pandemic: An intuitionistic fuzzy DEMATEL analysis. *Socio-Econ. Plan. Sci.* **2020**, *72*, 100911. [CrossRef]

40. Ren, Z.; Liao, H.; Liu, Y. Generalized Z-numbers with hesitant fuzzy linguistic information and its application to medicine selection for the patients with mild symptoms of the COVID-19. *Comput. Ind. Eng.* **2020**, *145*, 106517. [CrossRef]

41. Li, X.; Liao, H.; Wen, Z. A consensus model to manage the non-cooperative behaviors of individuals in uncertain group decision making problems during the COVID-19 outbreak. *Appl. Soft Comput.* **2021**, *99*, 106879. [CrossRef]

42. Shaban, W.M.; Rabie, A.H.; Saleh, A.I.; Abo-Elsoud, M.A. Detecting COVID-19 patients based on fuzzy inference engine and Deep Neural Network. *Appl. Soft Comput.* **2021**, *99*, 106906. [CrossRef] [PubMed]

43. Aggarwal, L.; Goswami, P.; Sachdeva, S. Multi-criterion intelligent decision support system for COVID-19. *Appl. Soft Comput.* **2021**, *101*, 107056. [CrossRef] [PubMed]

44. Ghorui, N.; Ghosh, A.; Mondal, S.P.; Bajuri, M.Y.; Ahmadian, A.; Salahshour, S.; Ferrara, M. Identifcation of dominant risk factor involved in spread of COVID-19 using hesitant fuzzy MCDM methodology. *Results Phys.* **2021**, *21*, 103811. [CrossRef] [PubMed]

45. Mishra, A.R.; Rani, P.; Krishankumar, R.; Ravichandran, K.S.; Kar, S. An extended fuzzy decision-making framework using hesitant fuzzy sets for the drug selection to treat the mild symptoms of Coronavirus Disease 2019 (COVID-19). *Appl. Soft Comput.* **2021**, *103*, 107155. [CrossRef]

46. Ecer, F.; Pamucar, D. MARCOS technique under intuitionistic fuzzy environment for determining the COVID-19 pandemic performance of insurance companies in terms of healthcare services. *Appl. Soft Comput.* **2021**, *104*, 107199. [CrossRef] [PubMed]

47. Sharma, M.K.; Dhiman, N.; Mishra, V.N. Mediative fuzzy logic mathematical model: A contradictory management prediction in COVID-19 pandemic. *Appl. Soft Comput.* **2021**, *105*, 107285. [CrossRef] [PubMed]

48. An, M.; Chen, Y.; Baker, C.J. A fuzzy reasoning and fuzzy analytical hierarchy process based approach to the process of railway risk information: A railway risk management system. *Inf. Sci.* **2011**, *181*, 3946–3966. [CrossRef]

49. Majumder, D.; Debnath, J.; Biswas, A. Risk analysis in construction sites using fuzzy reasoning and fuzzy analytic hierarchy process. *Procedia Technol.* **2013**, *10*, 604–614. [CrossRef]

50. An, M.; Lin, W.; Stirling, A. Fuzzy-reasoning-based approach to qualitative railway risk assessment. *Proc. Inst. Mech. Eng. Part F J. Rail Rapid Transit* **2006**, *220*, 153–167. [CrossRef]

51. Tong, Y.; Ma, Y.; Liu, H.M. The short-term impact of COVID-19 epidemic on the migration of Chinese urban population and the evaluation of Chinese urban resilience. *Acta Geogr. Sin.* **2020**, *75*, 2506–2520.

52. Lau, H.; Khosrawipour, V.; Kocbach, P.; Mikołajczyk, A.; Schubert, J.; Bania, J.; Khosrawipour, T. The positive impact of lockdown in Wuhan on containing the COVID-19 outbreak in China. *J. Travel Med.* **2020**, *27*, 1–7. [CrossRef]

53. Helena, B.; Jean, R.; Vanessa, S.; Désirée, N. A study of changes in everyday mobility during the Covid-19 pandemic: As perceived by people living in Malm, Sweden. *Transp. Policy* **2021**, *106*, 109–119.